New Semiconductors for High-Efficiency Solar Cells

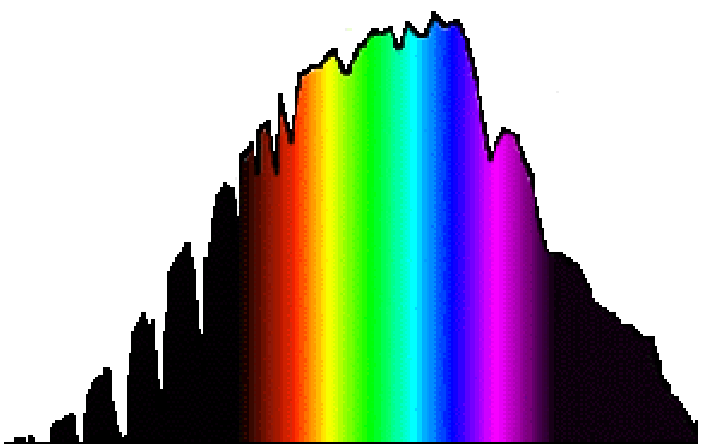

Wladek Walukiewicz

**Materials Sciences Division,
Lawrence Berkeley National Laboratory,
Berkeley, CA 94720**

Collaborators

- K. M. Yu, J. W. Ager III, J. Wu, W. Shan, O. Dubon, J. Beeman, E. Haller, Z Liliental-Weber
- K. Alberi, R. Jones, X. Li, N. Miller, D. Yamaguchi
- Hai Lu and William J. Schaff, Cornell University; P. Becla, MIT; A. Ramdas, Purdue University, J. F. Geisz, NREL

➢ *Support:*
  - *DOE Contract No. DE-AC03-76SF00098;*
  - *US NSF DMR-0109844;*
  - *ONR Contract No. N000149910936*
  - *NRO*

Outline

- The big picture
- Solar cell fundamentals
- Multijunction cells: group III-nitrides
- Multiband cells: highly mismatched alloys
- Solar splitting of water

The first Si cell

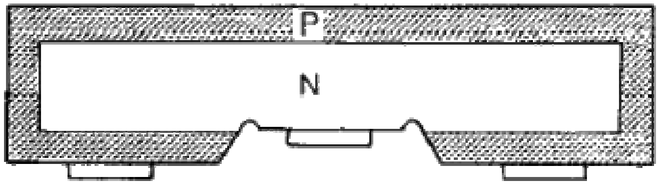

D.M. Chapin (center), C.S. Fuller (right) and G.L. Pearson (left), "A New Silicon P-N Junction Photocell for Converting Solar Radiation into Electrical Power", J. Appl. Phys. **25** 676 (1954).

The New York Times: April 26, 1954
"Vast Power is Tapped by Battery Using Sand Ingredient"

…may mark the beginning of a new era, leading eventually to the realization of one of mankind's more cherished dream —the harnessing of the almost limitless energy of the sun for the uses of civilisation".

A. Luque, GRC, NH

Mean Global Energy Consumption, 1998

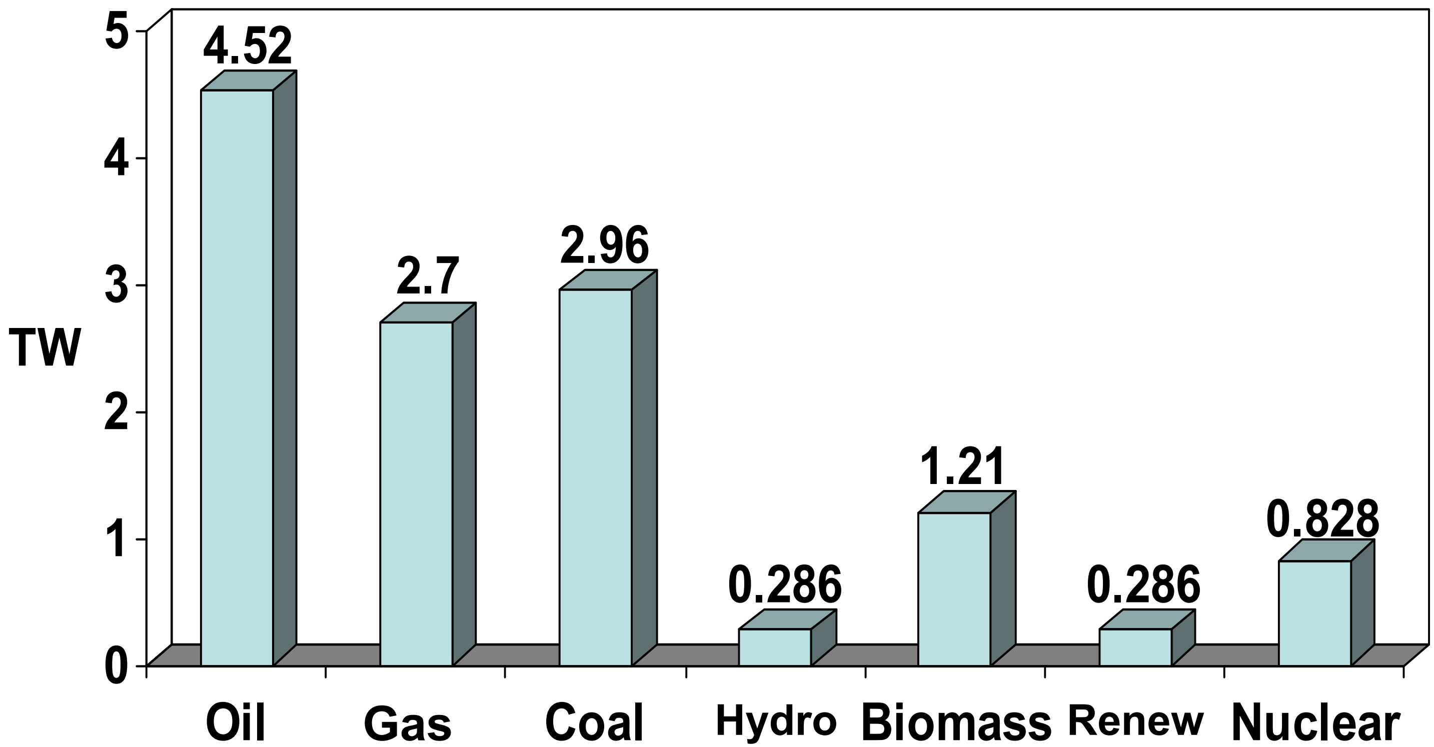

Total: 12.8 TW U.S.: 3.3 TW (99 Quads)

N. Lewis, DOE workshop

Solar Energy Potential

- Theoretical: 1.2×10^5 TW solar energy potential

  (1.76×10^5 TW striking Earth; 0.30 Global mean)

  - Energy in 1 hr of sunlight ↔ 14 TW for a year

- Practical: ≈ 600 TW solar energy potential

  (50 TW - 1500 TW depending on land fraction etc.; WEA 2000)

  Onshore electricity generation potential of ≈60 TW (10% conversion efficiency):

- *Photosynthesis*: 90 TW

Solar Land Area Requirements

Solar Land Area Requirements

6 Boxes at 3.3 TW Each

World PV Cell/Module Production (MW)

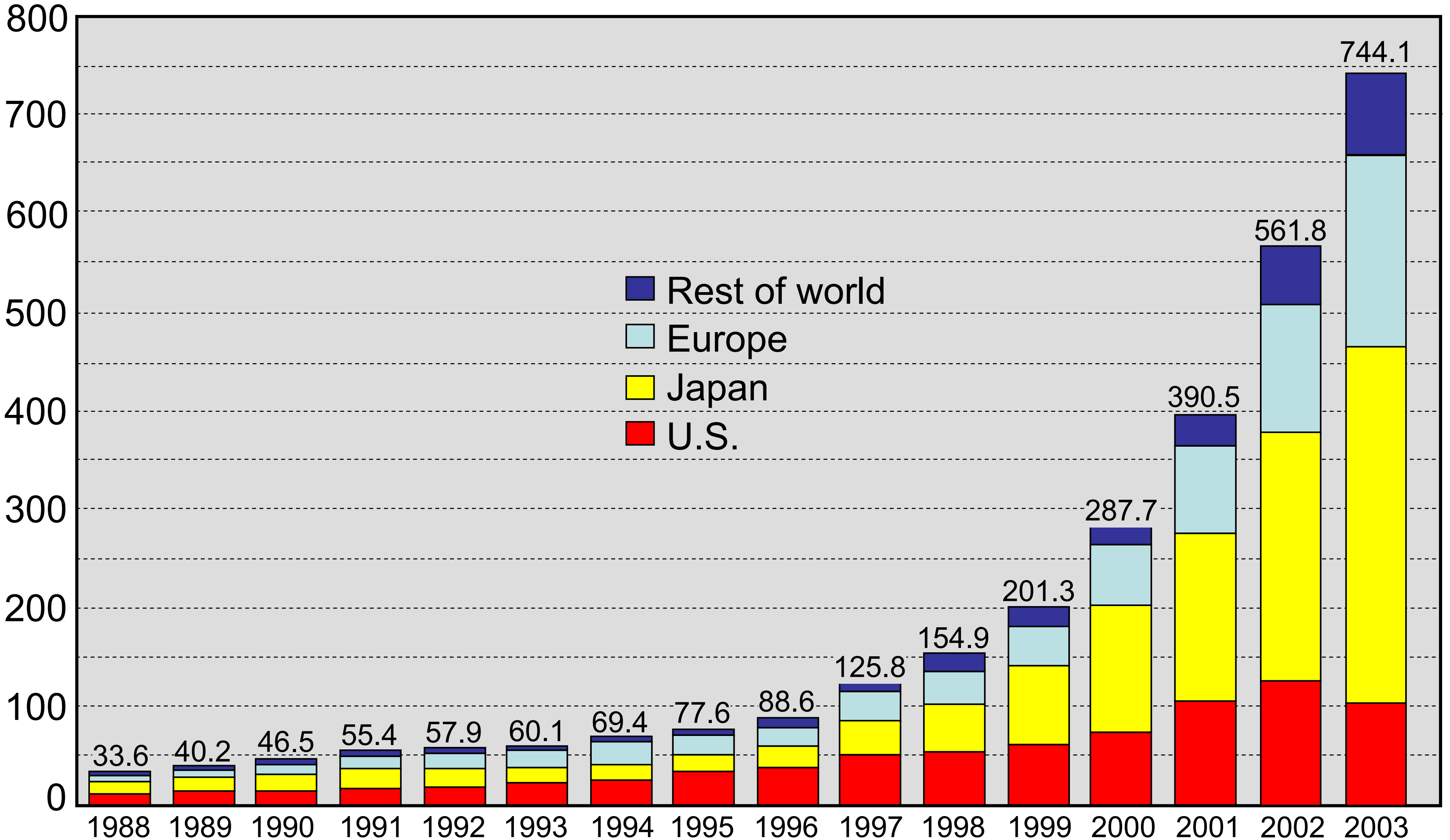

Source: *PV News*, March 2004

2004: 1200 MW

Today: Production Cost of Electricity (in the U.S. in 2002)

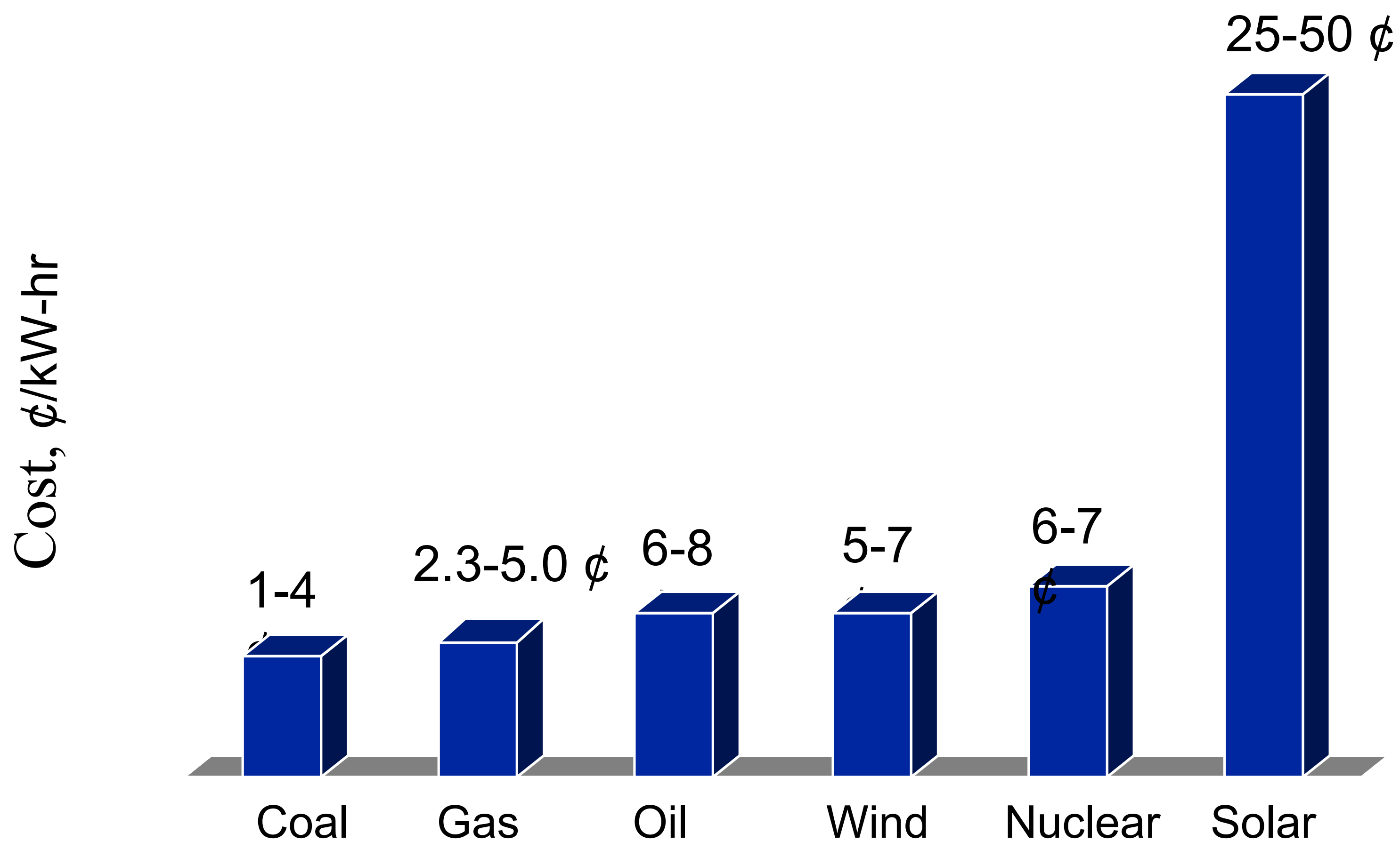

Energy Pay-back Time for PV Cells

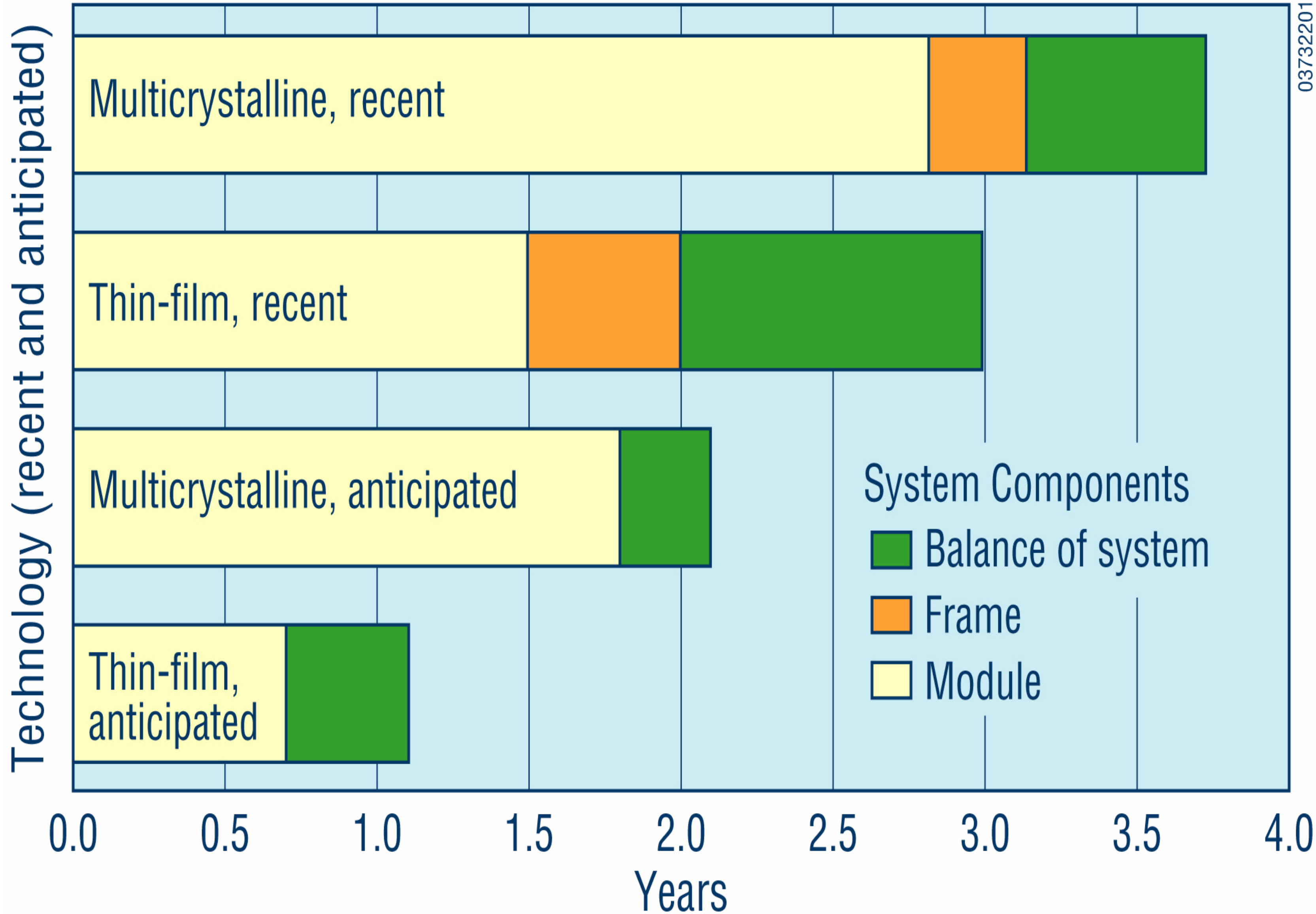

THE SOLAR CHALLENGE

- With a projected global population of 12 billion by 2050 coupled with moderate economic growth, the total global energy consumption is estimated to be ~28 TW. Current global use is ~13 TW.
- To cap CO_2 at 550 ppm (twice the pre-industrial level), most of this additional energy needs to come from carbon-free sources.
- Solar energy is the largest non-carbon-based energy source (100,000 TW).
- However, it has to be converted at reasonably low cost.

A. Nozik, DOE workshop

Best Research-Cell Efficiencies

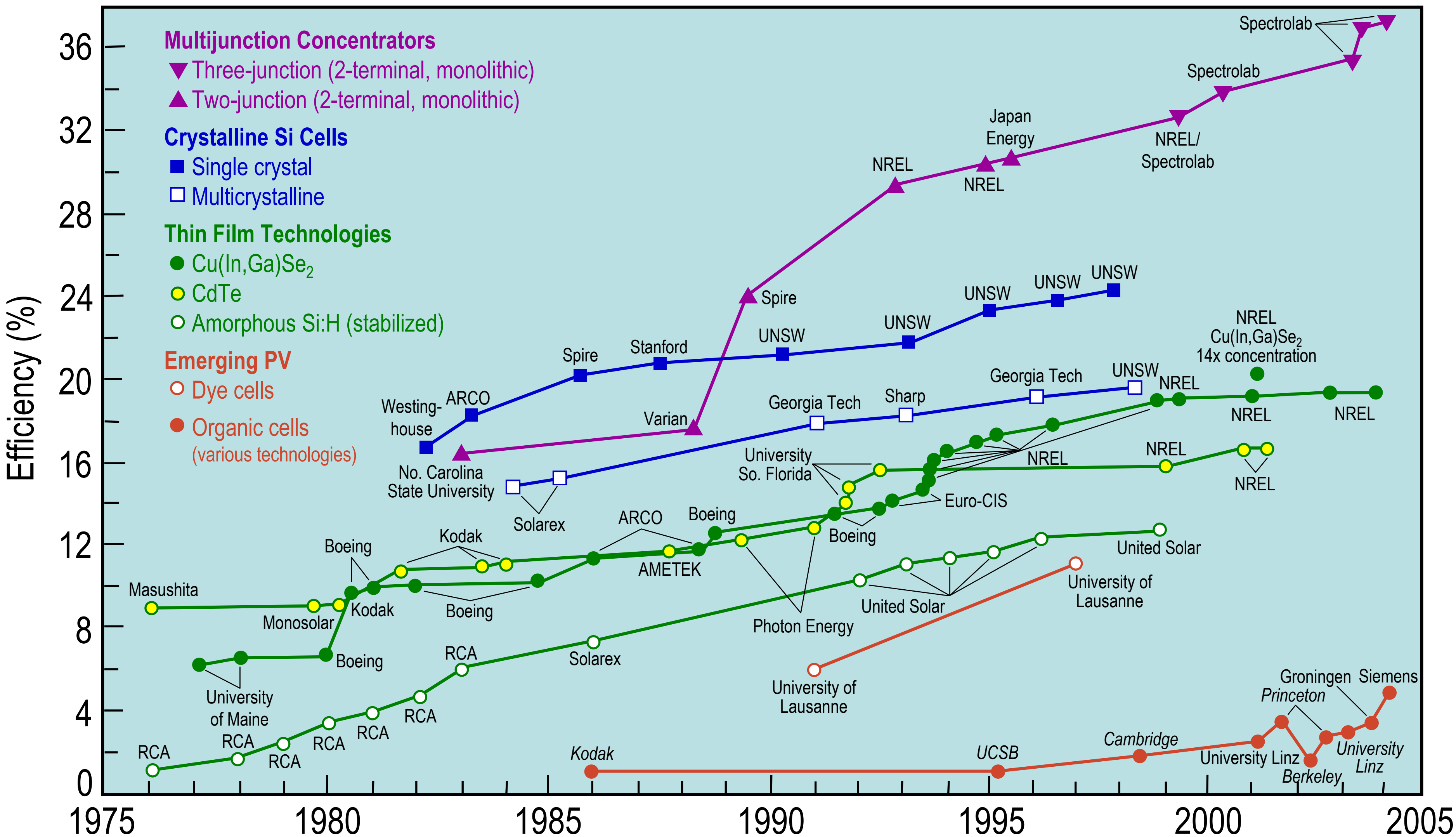

Best Research-Cell Efficiencies

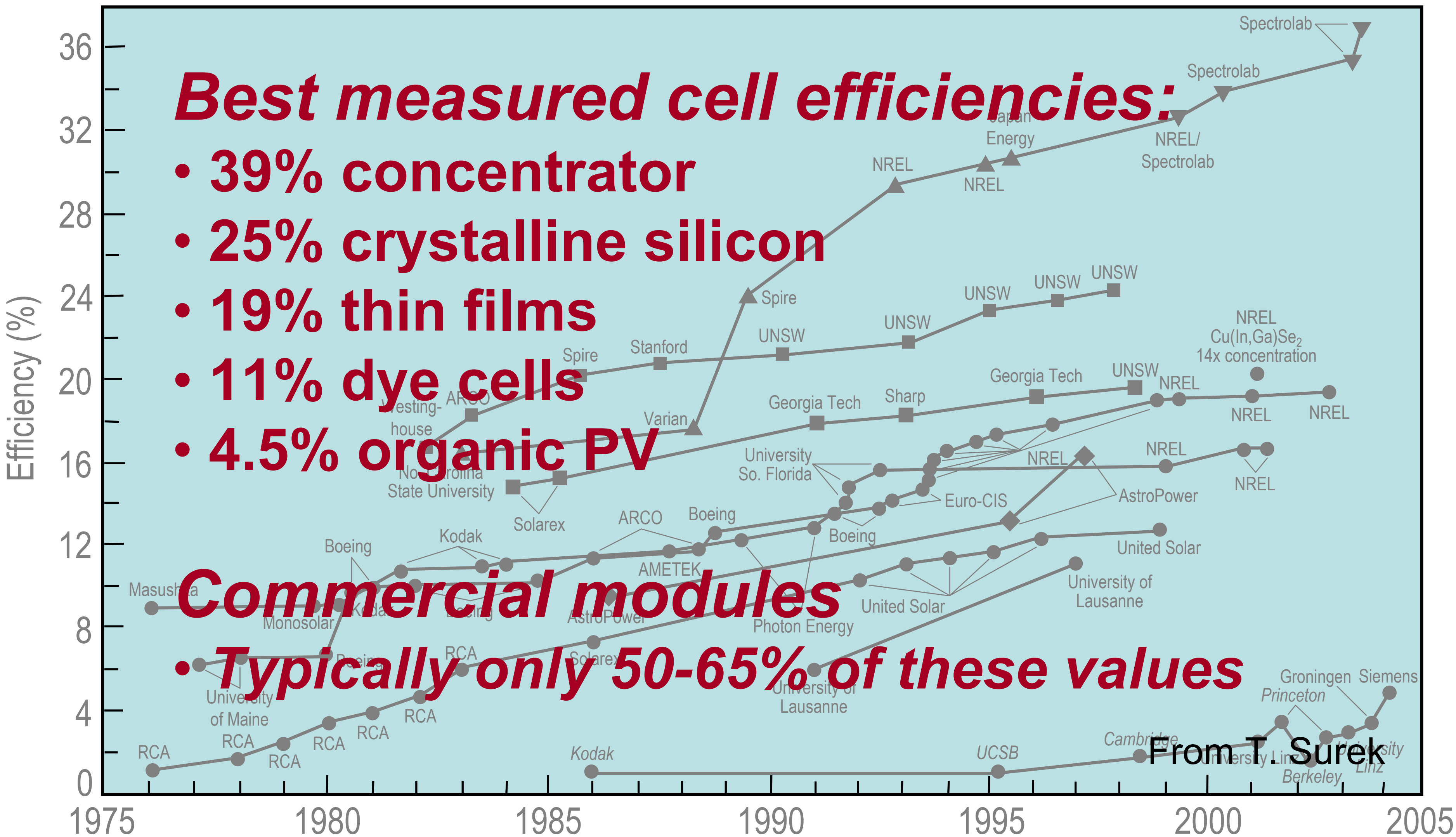

Best measured cell efficiencies:

- **39% concentrator**
- **25% crystalline silicon**
- **19% thin films**
- **11% dye cells**
- **4.5% organic PV**

Commercial modules

- ***Typically only 50-65% of these values***

Fundamentals of Photovoltaics

1. **Thermalization loss**
2. **Junction loss**
3. **Contact loss**
4. **Recombination loss**

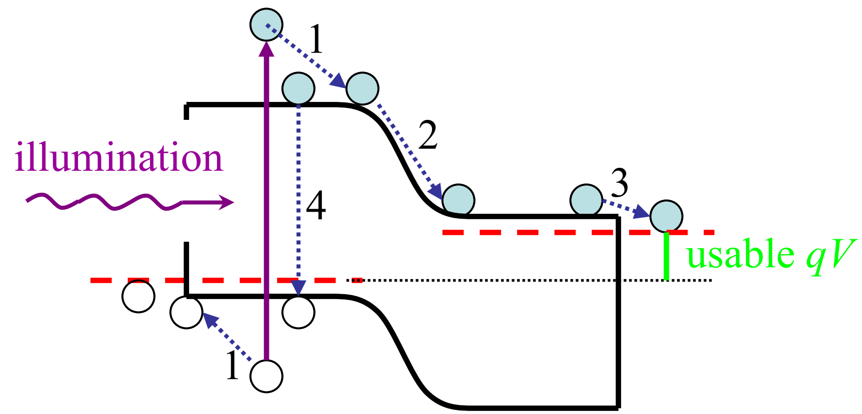

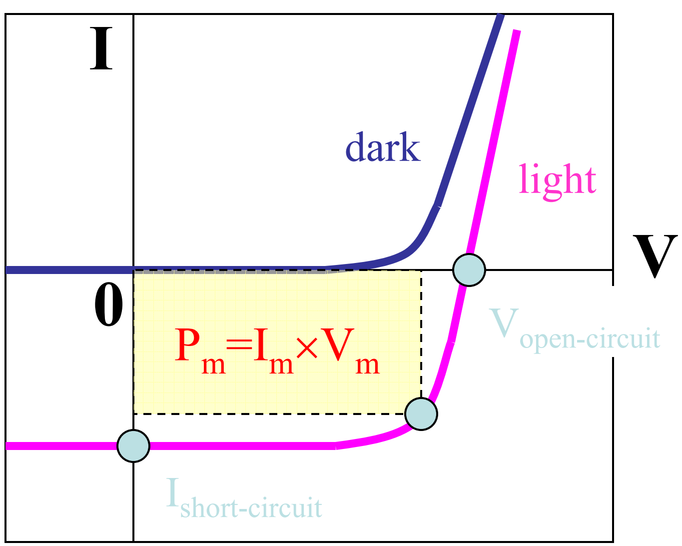

- **Dark and light I-V curves**
- **$V_{open\text{-}circuit}$**
- **$I_{short\text{-}circuit}$**
- **Maximum power P_m**
- **Fill factor (squareness)**

$FF = P_m / (V_{open\text{-}circuit} \times I_{short\text{-}circuit})$

Multijuction solar cells

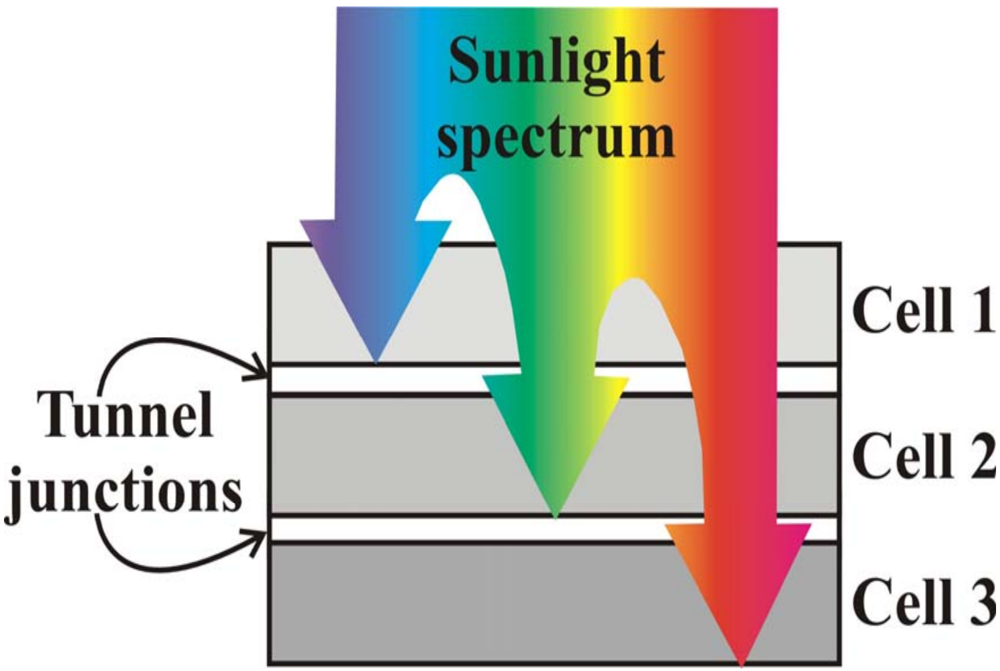

Larger open circuit voltage

- A stack of single gap solar cells.
- Each of the cells uses different part of solar spectrum.
- The open circuit voltage is the sum of the V_{OC}'s of individual cells.
- Requires current matching.

State-of-the-art 3-Junction Solar Cells

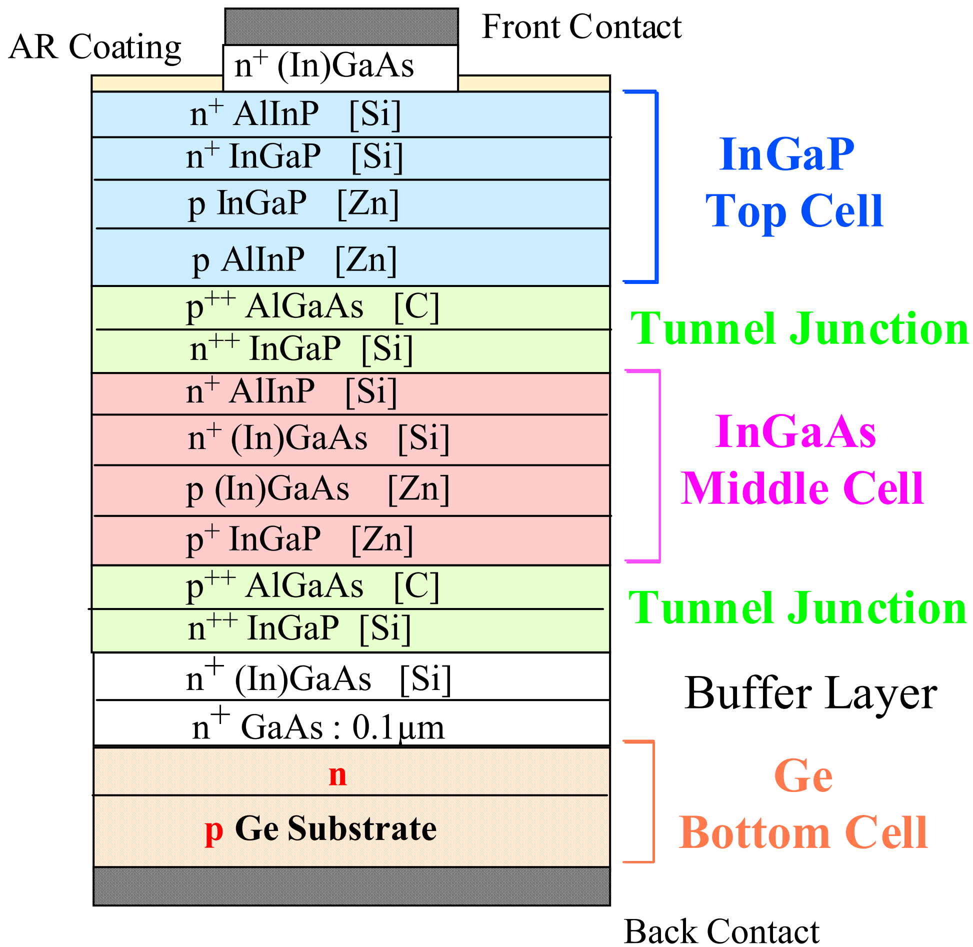

- **Efficiencies up to 39%**
- **Six different elements**
- **Three different dopants**
- **Practically used: 3-junction cells**
- **Research: 4 to 5 junctions**

Yamaguchi et. al., 2003 Space Power Workshop

Group III-Nitrides before 2002

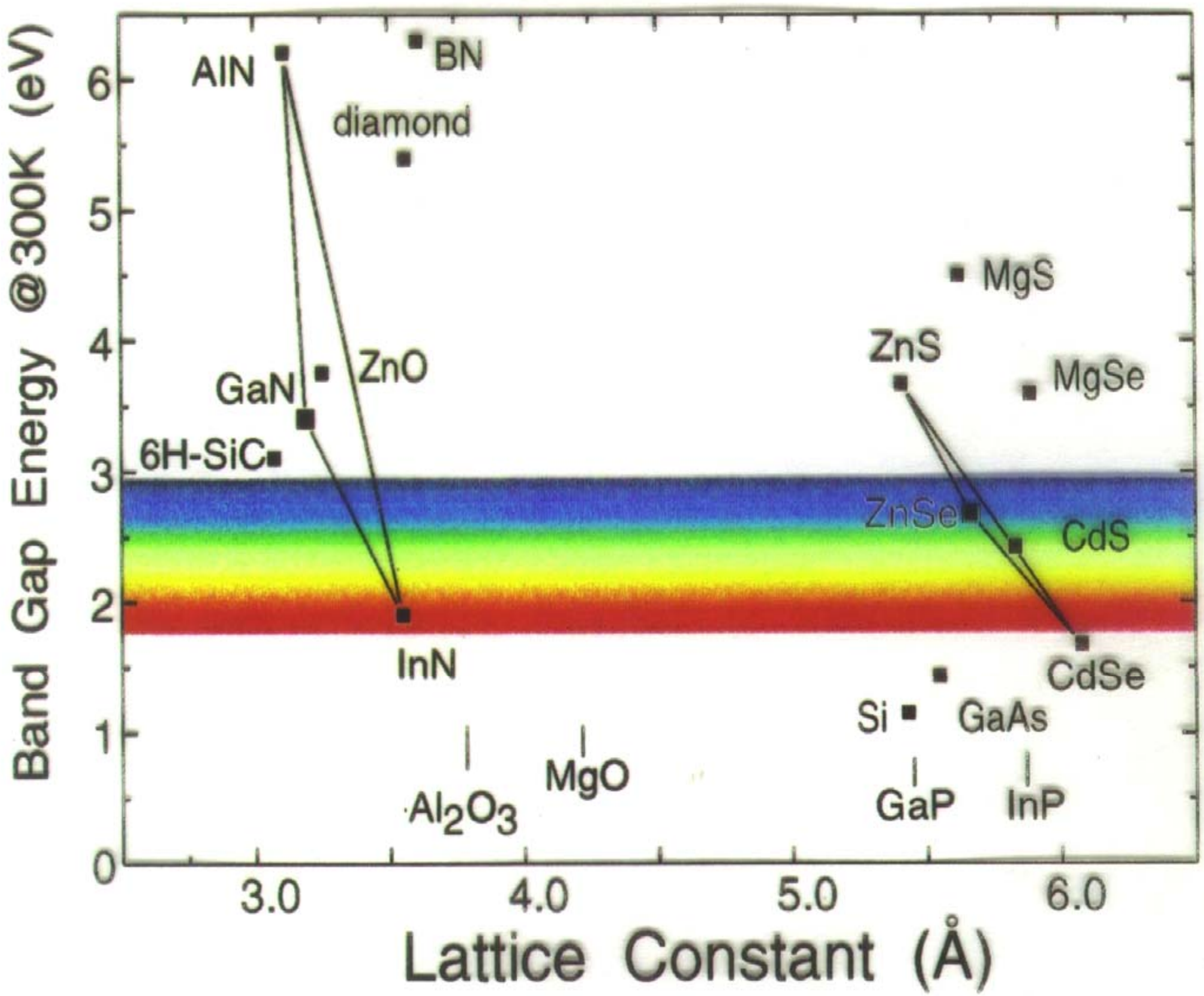

Fundamental Bandgap of Wurtzite InN

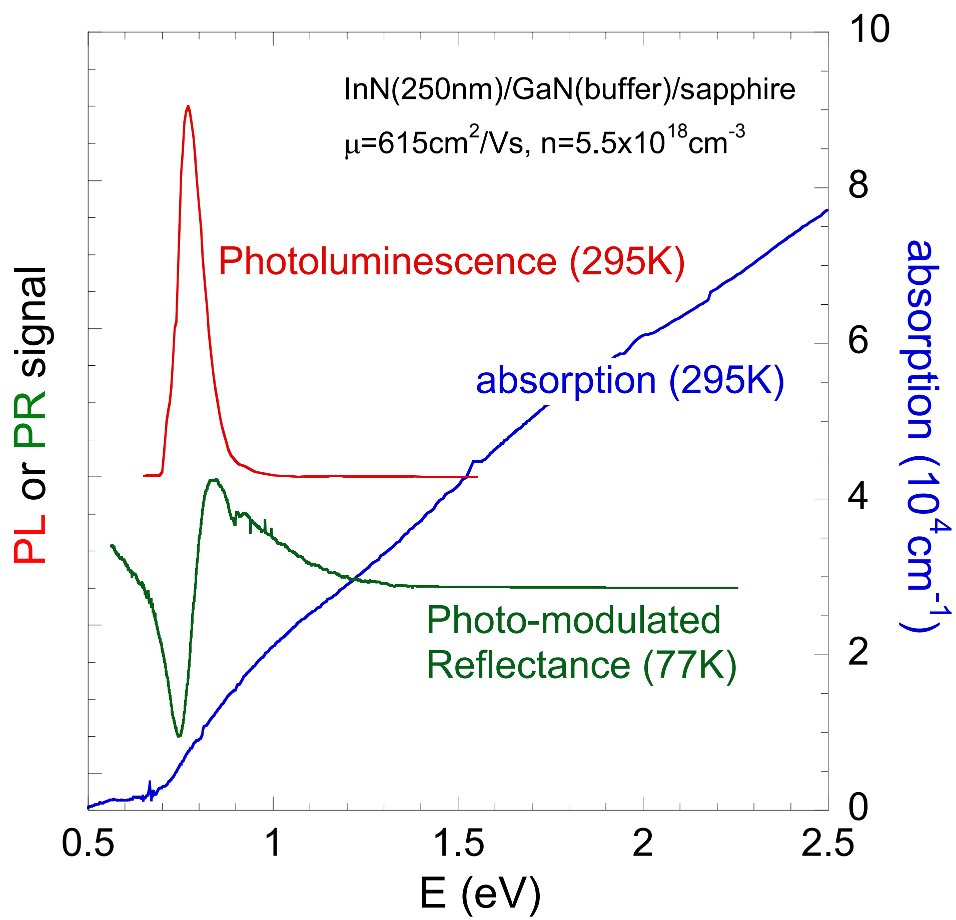

- MBE-grown high-quality InN
- All characteristic band gap features lie near 0.7 eV
- No energy gap is observed around 2 eV

$In_{1-x}Ga_xN$ Alloys

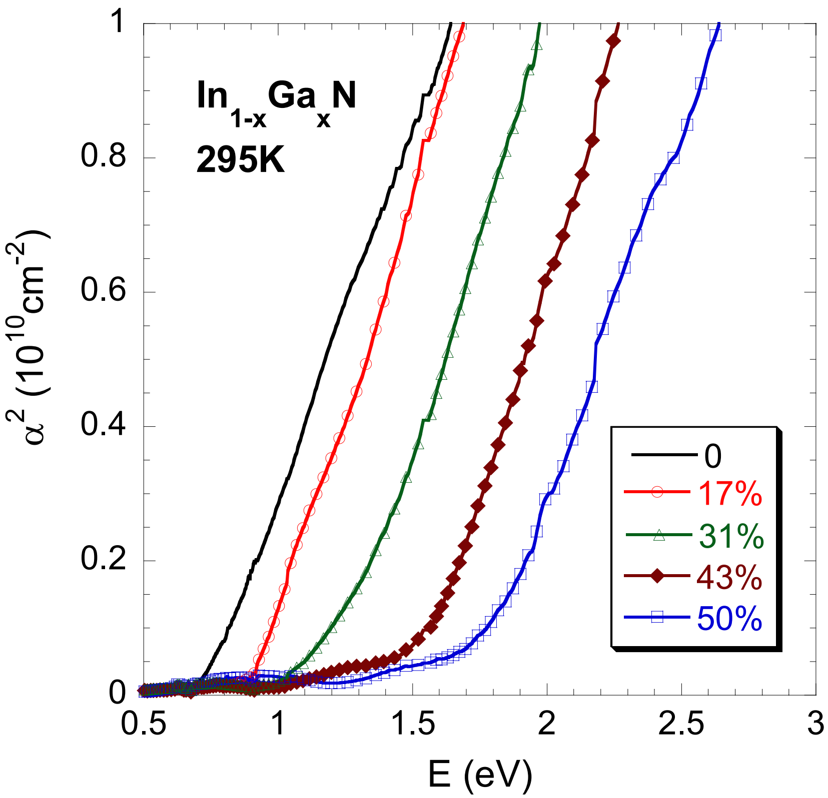

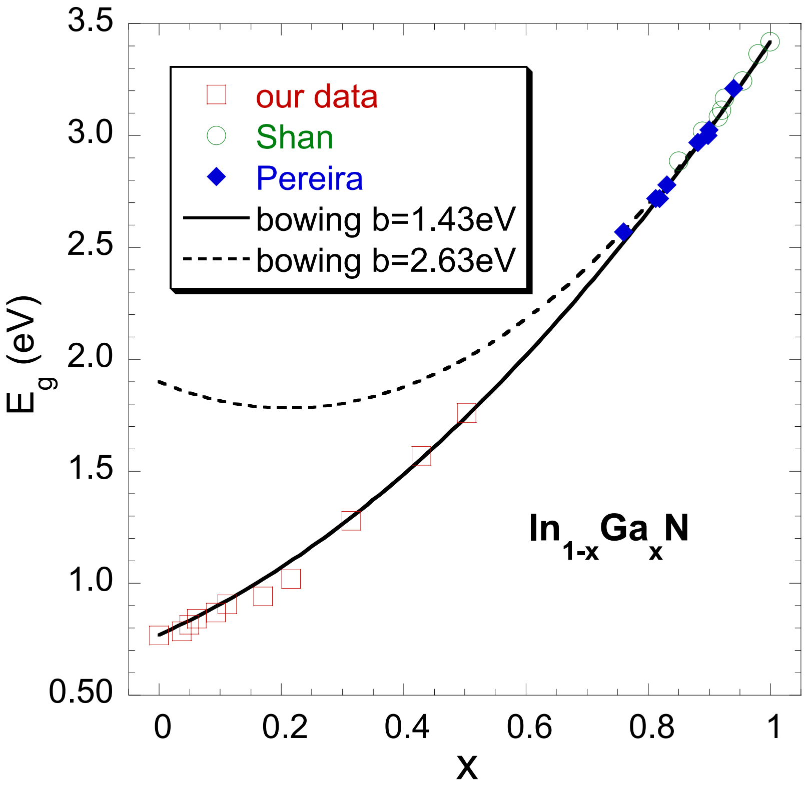

- Small bowing parameter in $In_{1-x}Ga_xN$: $b = 1.43$ eV
- The bandgap of this ternary system ranges from the infrared to the ultraviolet region!

Full solar spectrum nitrides

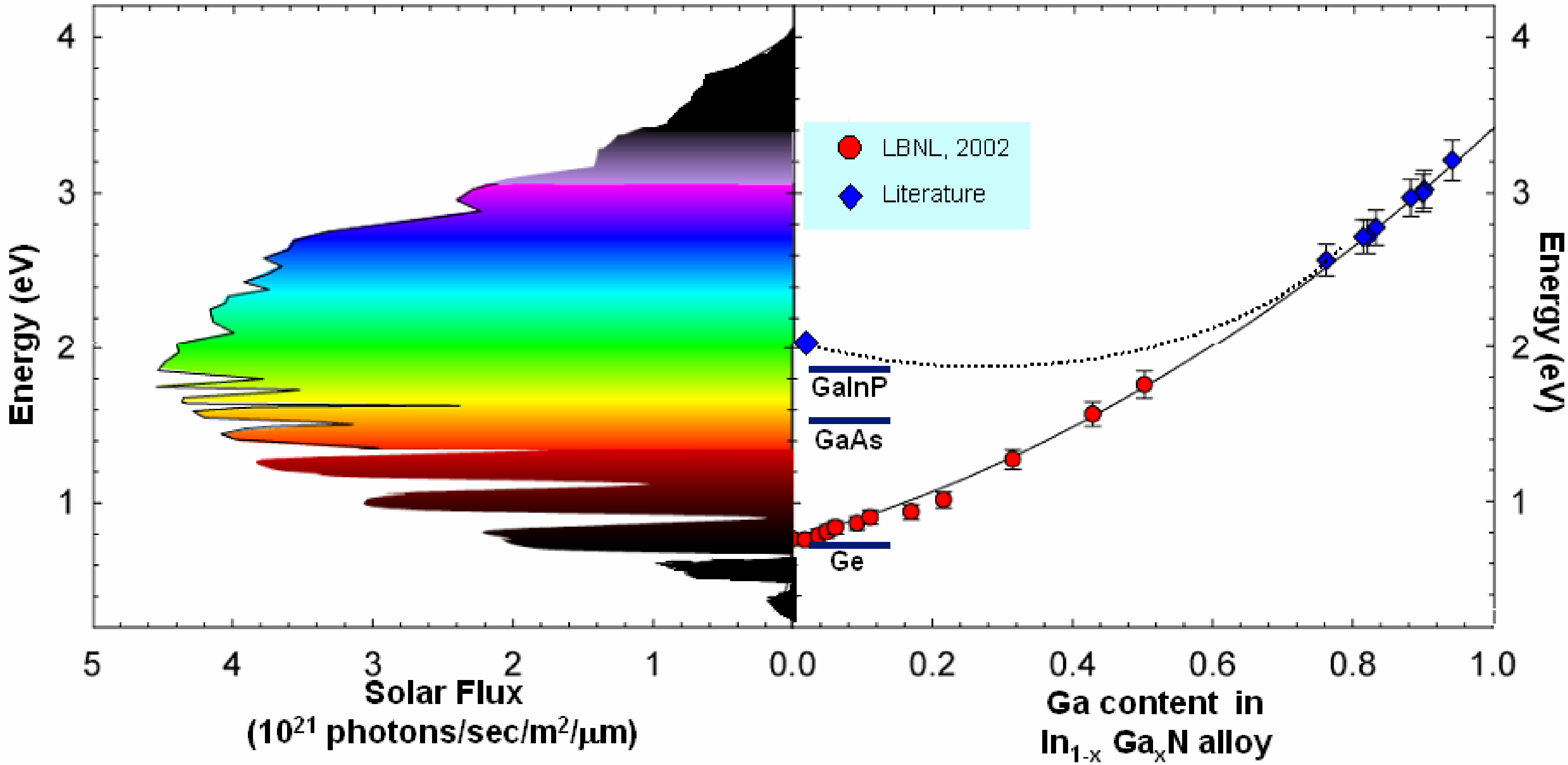

- The direct energy gap of $In_{1-x}Ga_xN$ covers most of the solar spectrum

Space Applications: Irradiation Effects

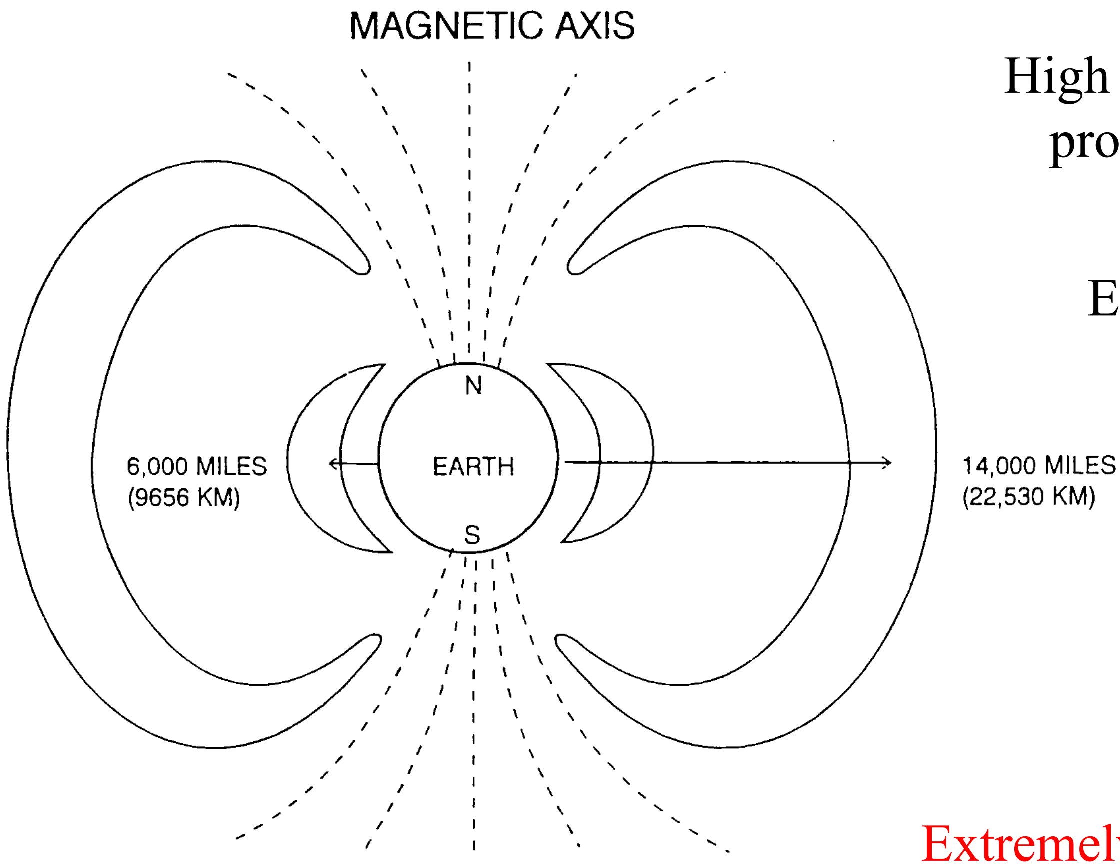

Van Allen belts

High density of electrons and protons, up to 10^8 $cm^{-2}s^{-1}$

Energies from keV to hundreds of MeV

Extremely hostile environment

High Energy Particle Irradiation

Kirtland AFB Dynamitron

1 MeV electrons up to 1×10^{17} cm^{-2}

LBNL van de Graaf accelerator

2 MeV protons up to 2×10^{15} cm^{-2}

2 MeV He^{+} up to 2×10^{15} cm^{-2}

LBNL ion implanter

200 keV Ne^{+}

NRL model used to put electron, proton, and alpha irradiation on same scale
Non-ionizing energy loss (NIEL) and displacement damage dose (Dd)

Effect of Irradiation on Photoluminescence Intensity

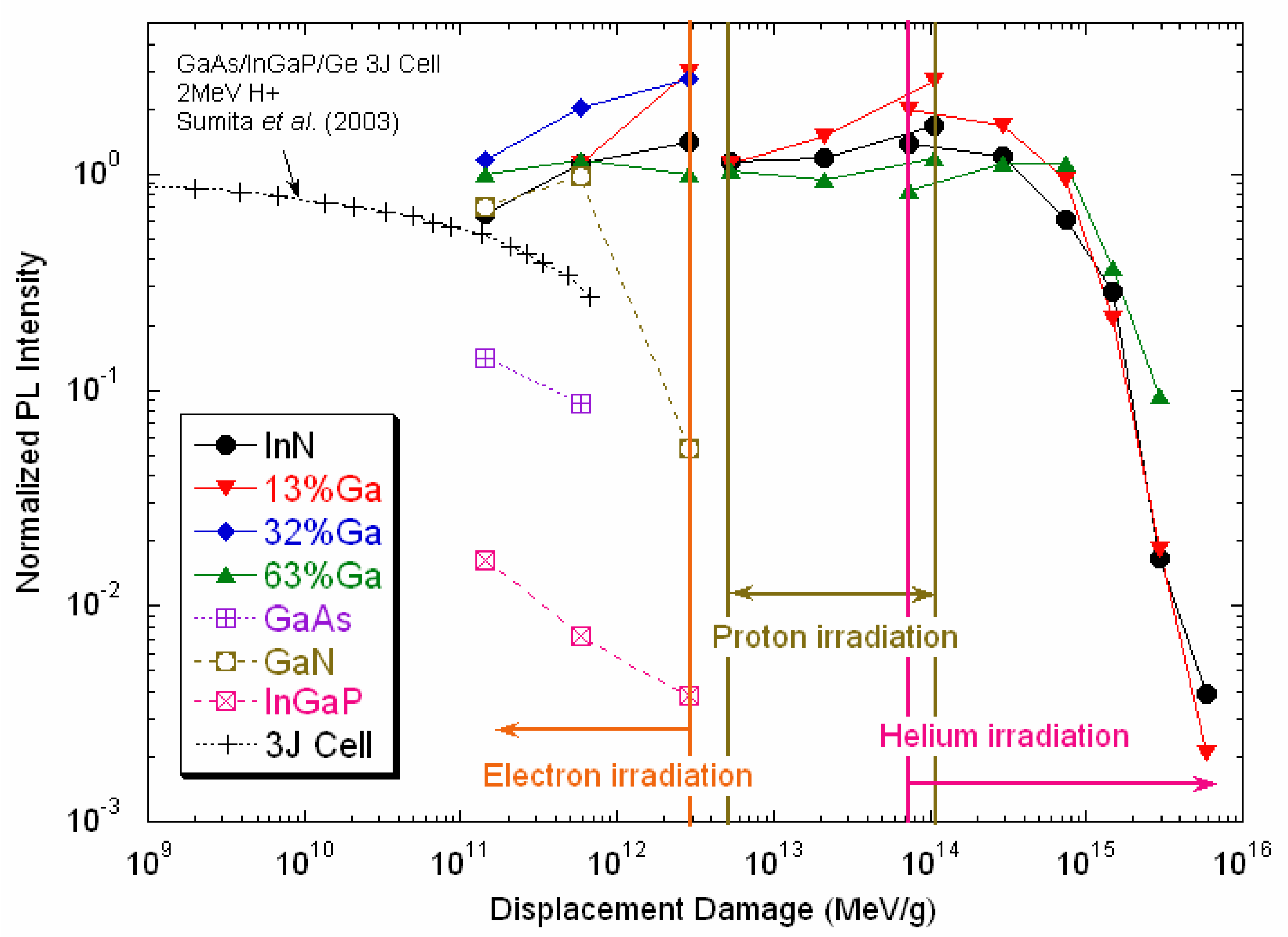

Surface Electron Accumulation

- Surface/interface native defects (such as dangling bonds) have similar energy to radiation-induced defects
- High concentration of defects near surface leads to Fermi level pinning
- Surface accumulation of electrons due to pinning, N_s=3.5x10^{13} cm^{-2}

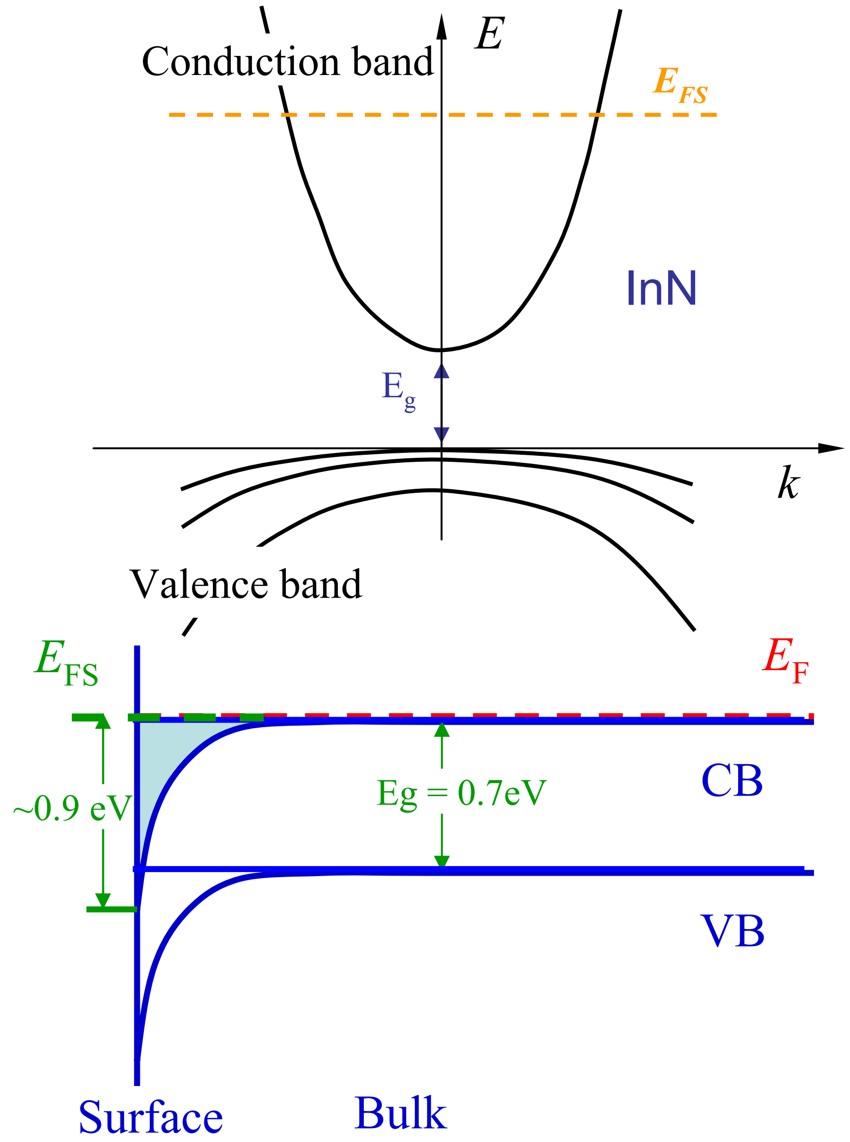

P-type doping of InN

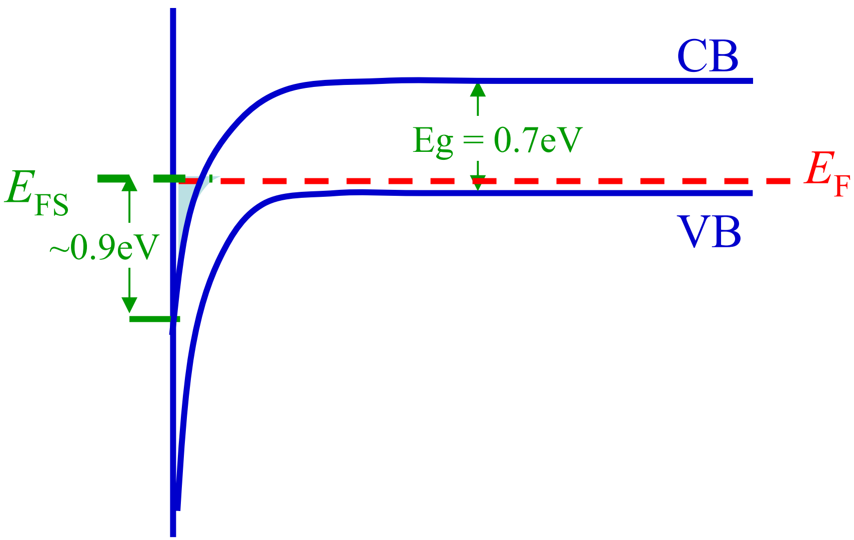

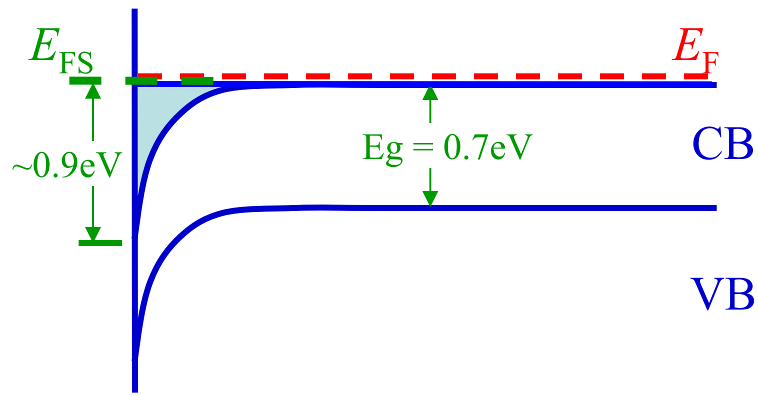

P-type InN

Hall effect measures the inversion layer only

No PL because of charge separation

N-type InN

Both surface accumulation layer and

bulk contribute to the conductivity.

The surface contribution is insignifcant

in samples thicker than 0.1 μm

CV: Mg-doped InN

can access p-type material under inversion layer

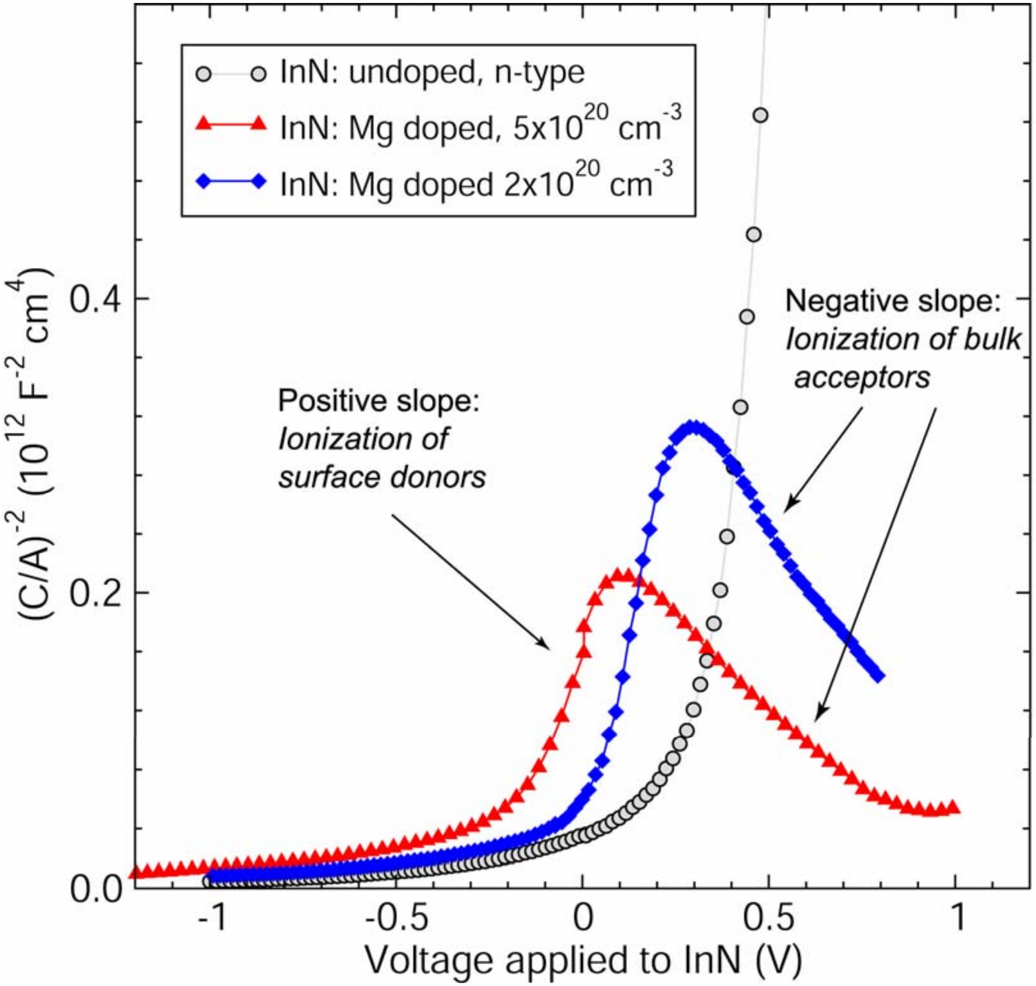

Slope change in plot consistent with surface inversion

Observed in all Mg-doped InN samples observed to date

The evidence for p-type InN is further supported by measurements of Hall effect and PL in irradiated samples

R. E. Jones, K. M. Yu, S. X. Li, W. Walukiewicz, J. W. Ager III, E. E. Haller, H. Lu, and W.J. Schaff, "Evidence for p-type doping of InN," Phys. Rev. Lett., in press.

InN and In-rich InGaN – issues and problems

- Origin of the large energy gap
- Extreme propensity for n-type doping
- P-type doping
- Properties of surfaces and interfaces

Multi-band Solar Cells (MBSC)

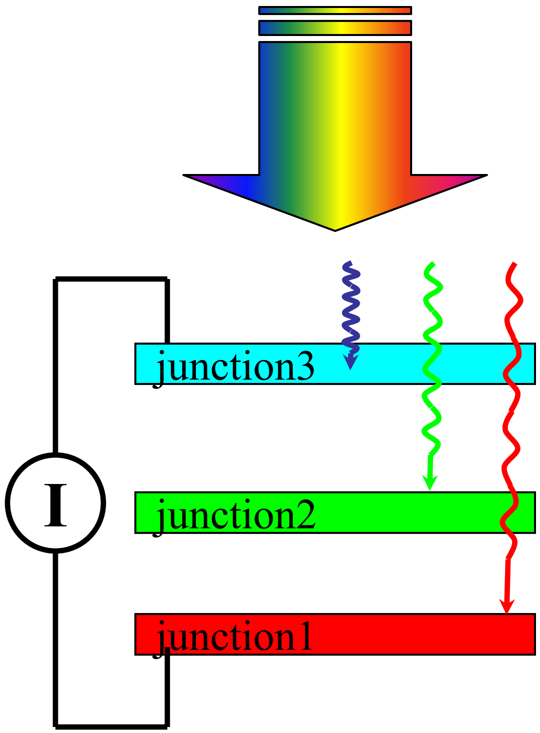

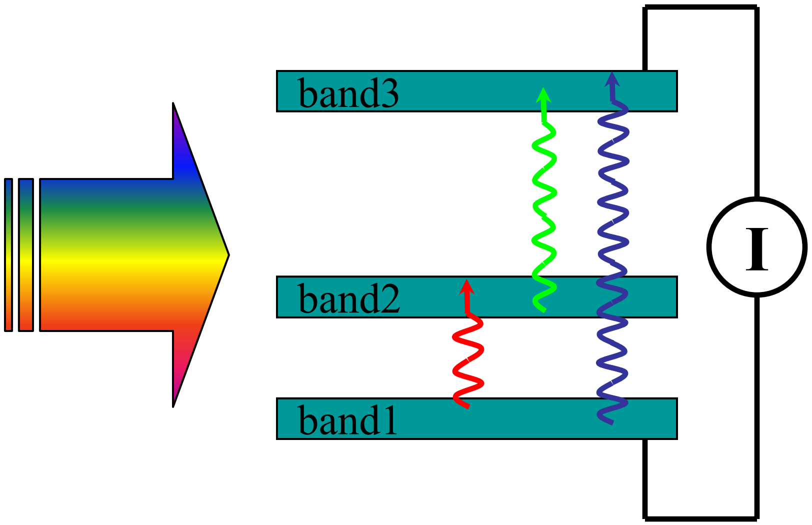

Multi-junction

- Single gap (two bands) each junction
- N junctions ⇒ N absorptions
- Add one junction ⇒ add one absorption

Multi-band

- Single junction (no lattice-mismatch)
- N bands ⇒ N·(N-1)/2 gaps
  ⇒ N·(N-1)/2 absorptions
- Add one band ⇒ add N absorptions

Intermediate band solar cells

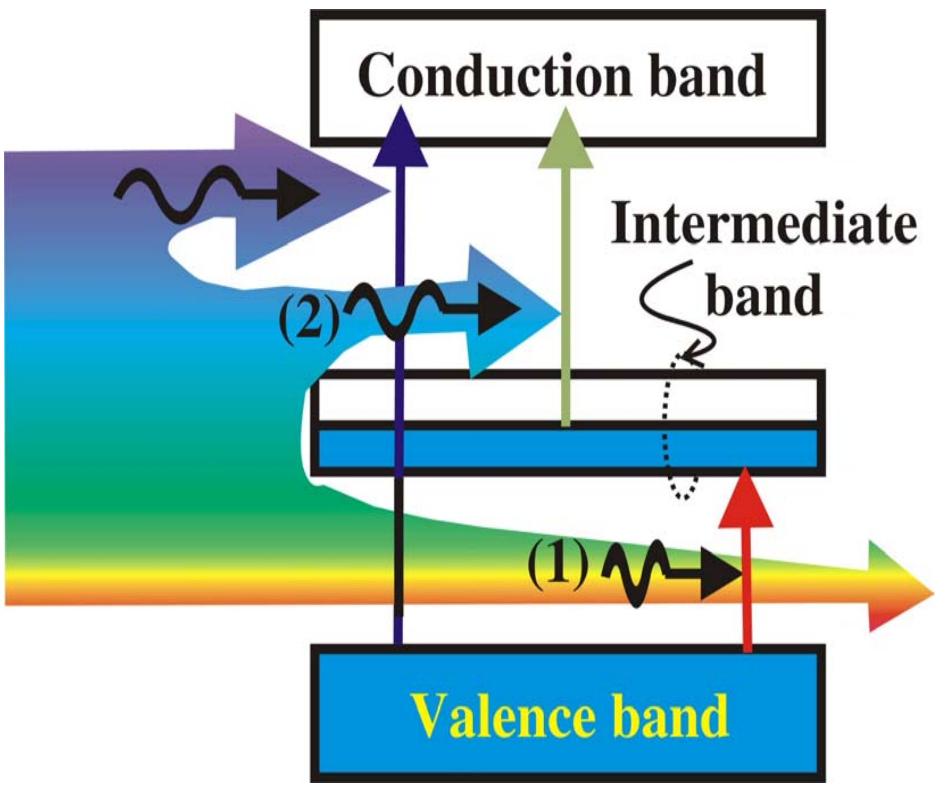

- Requires a partially occupied intermediate band.
- The intermediate band utilizes low energy photons serving as a “stepping stone”.
- Increases the current without decreasing the open circuit voltage.

Intermediate Band Cell

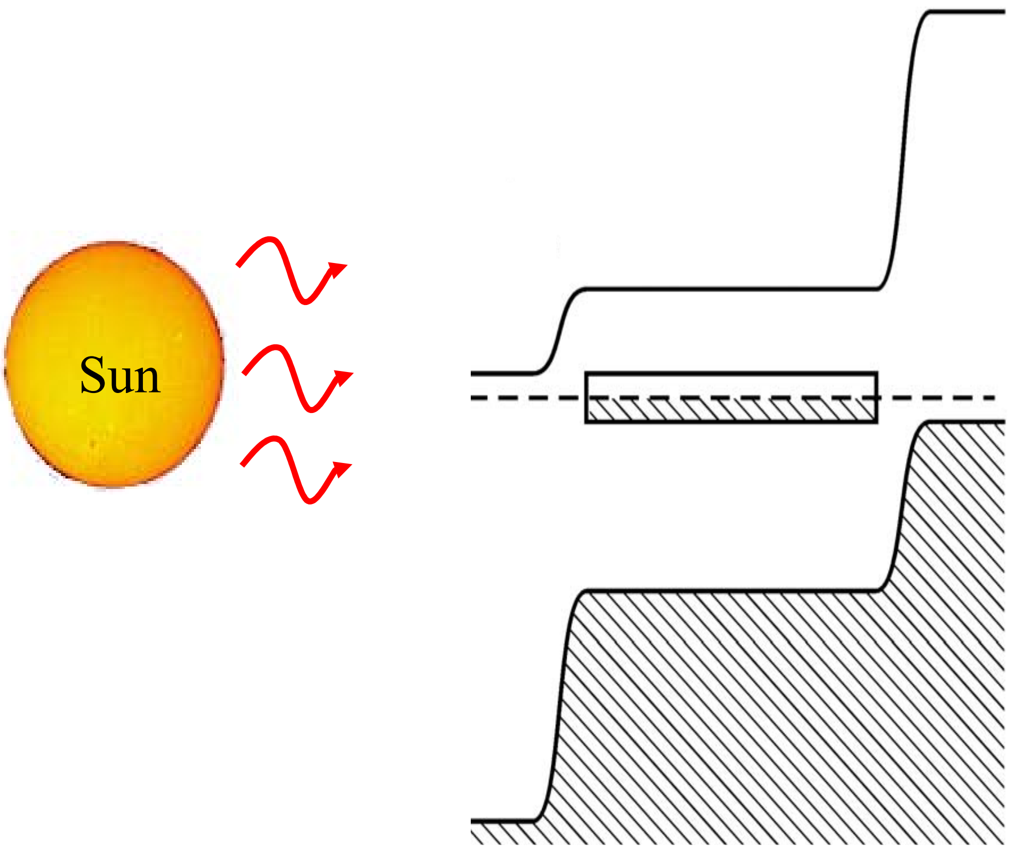

L. Cuadra, et. al., Thin Solid Films, 451-452, 593 (2004)

Intermediate Band Cell

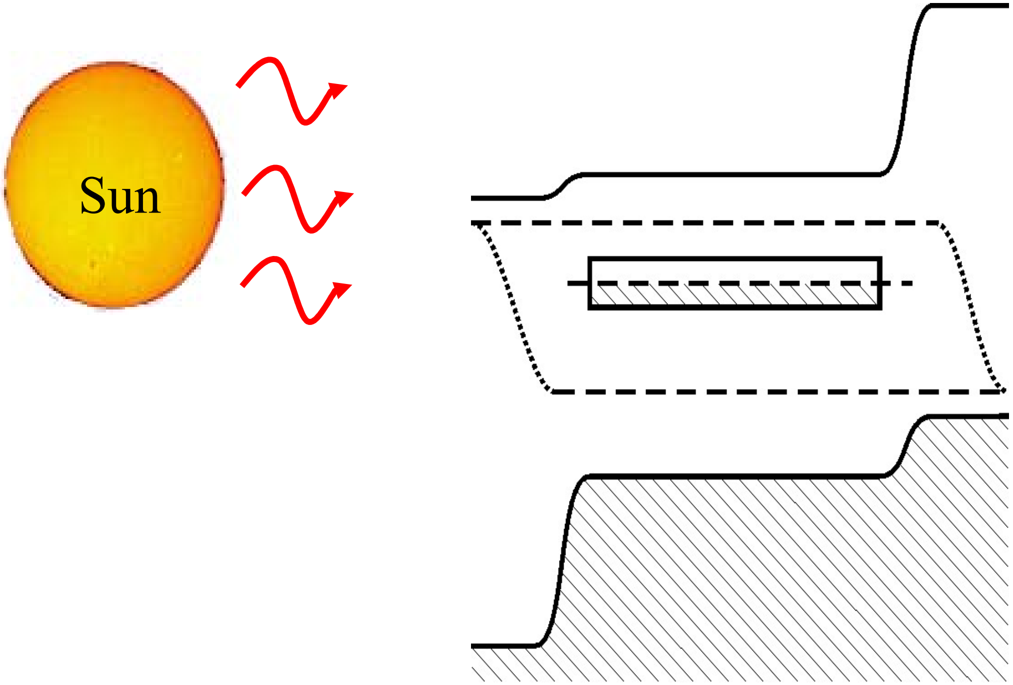

Intermediate Band Cell

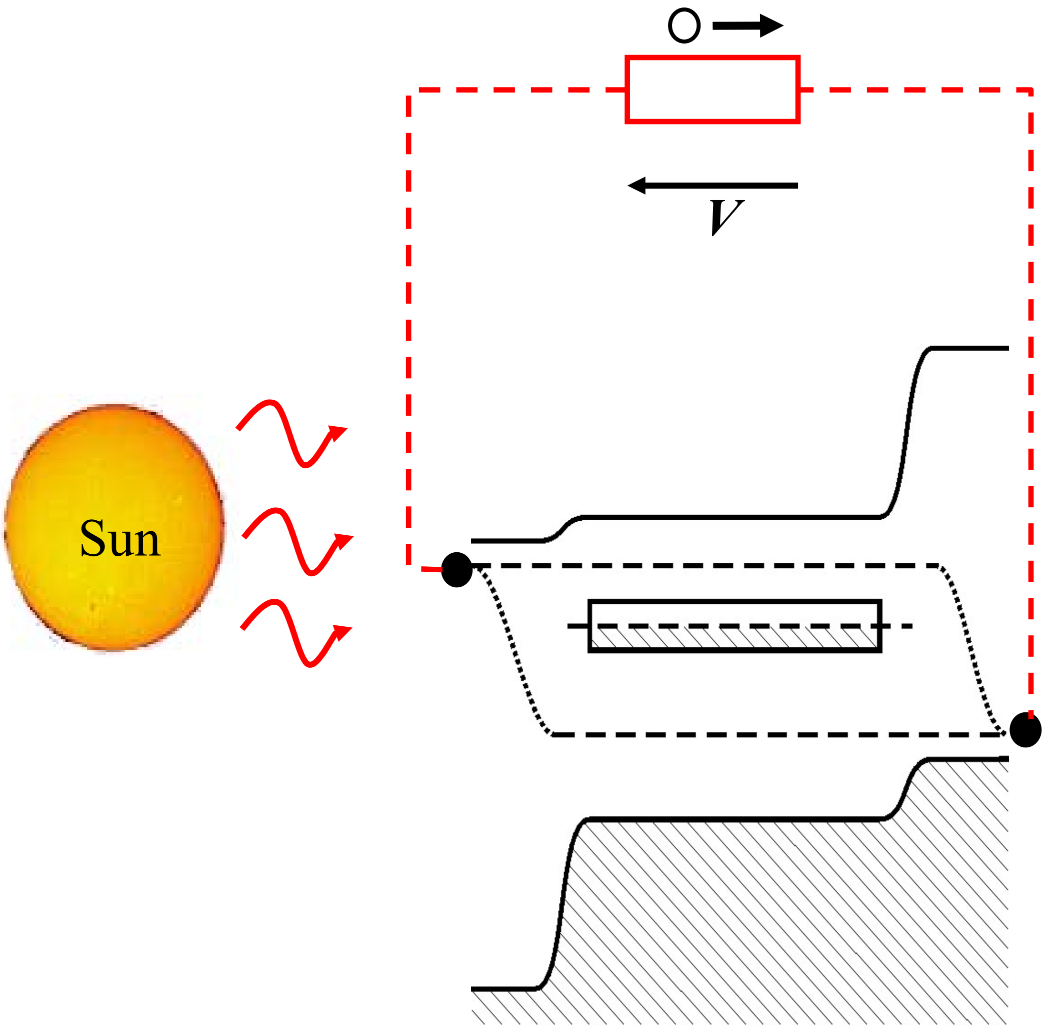

Numerical Calculation of the Thermodynamic Limit of the Efficiency of MBSC

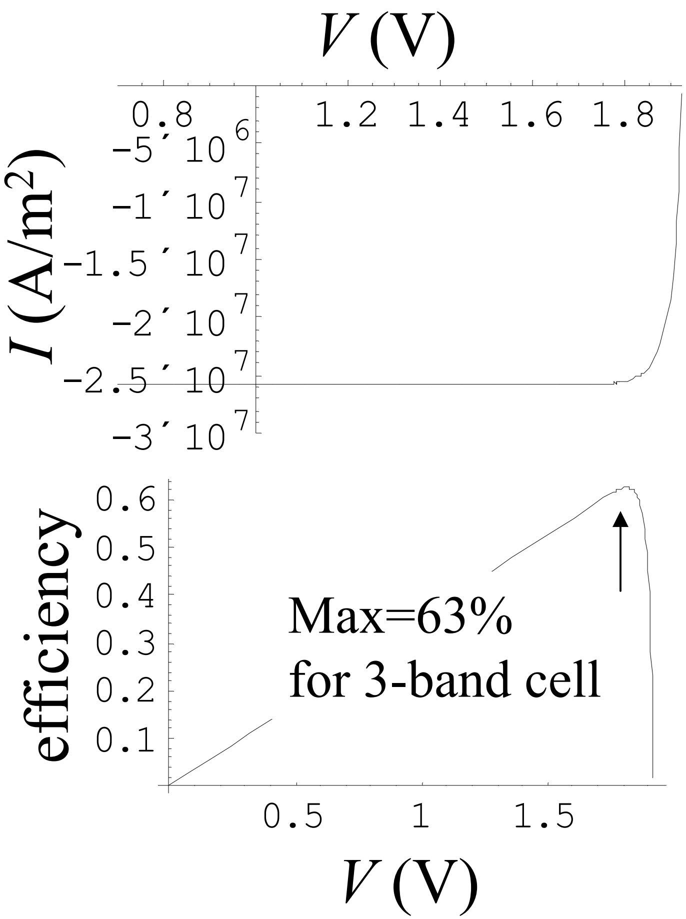

Maximum efficiency is 72% for 4-band cell.

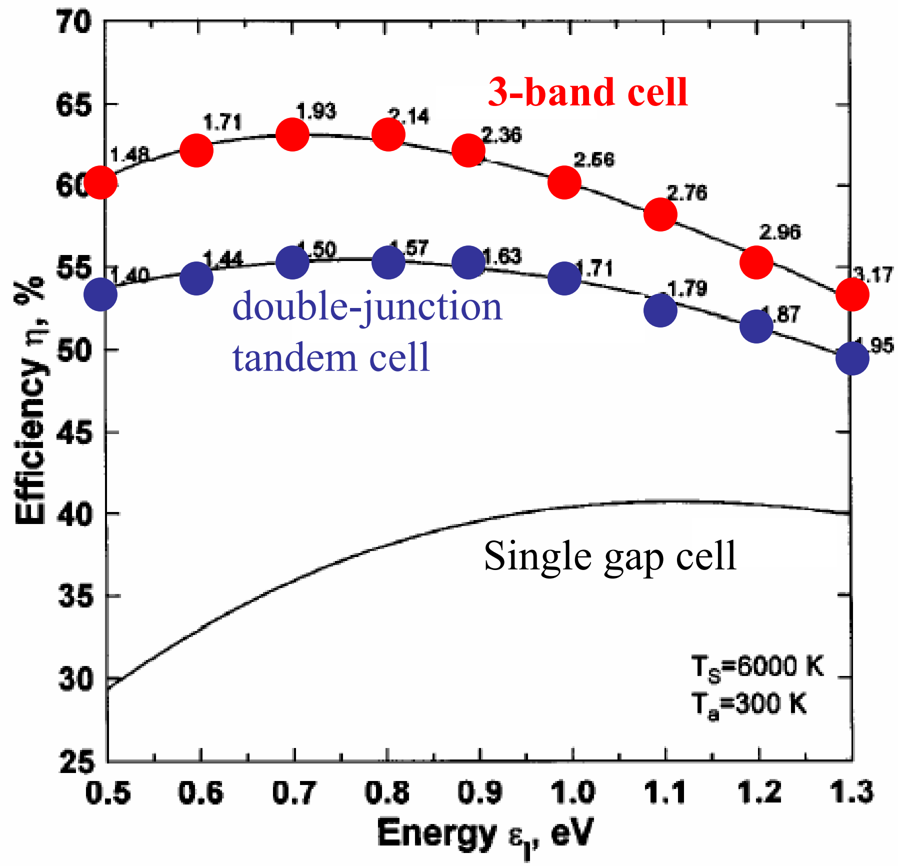

FIG. 2. Efficiency limit for a solar cell with an intermediate band and for a two-terminal ideal tandem cell, in both cases vs the lowest band gap ϵ_I, and for a cell with a single band gap. The corresponding values of the highest band gap in cells with intermediate band (E_G) and in tandem cells (E_C), for maximum efficiency, are also presented.

Well matched semiconductor alloys

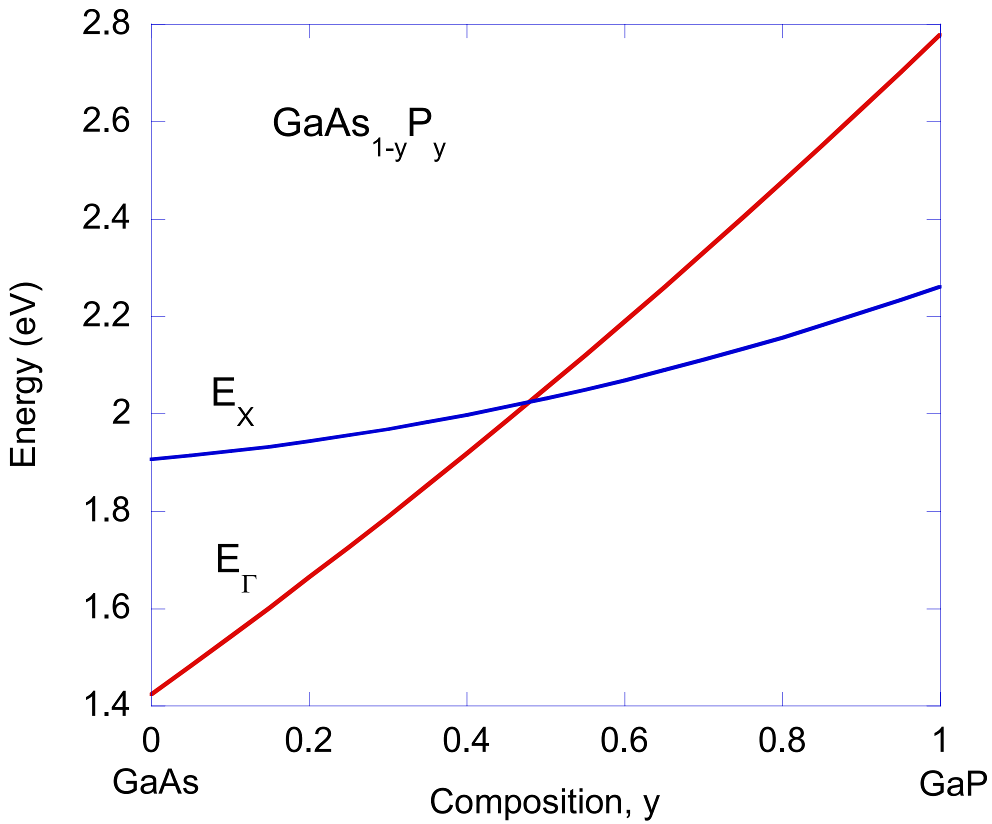

- Well explained by the virtual crystal approximation
- Nearly linear composition dependence of all critical point energies of the electronic band structure
- Small bowing of the fundamental band gap
- Widely used to tune bandgaps – lasers, LEDs, etc.
- Relatively easy to synthesize in the whole composition range

Highly Mismatched Alloys (HMAs)

Electronegativities, X and atomic radii, R

IV	V	VI
C 2.6	N X=3.0 R=0.075 nm	O X=3.4 R=0.073 nm
Si 1.9	P X=2.2 R=0.12 nm	S X=2.6 R=0.11 nm
Ge 2.0	As X=2.2 R=0.13 nm	Se X=2.6 R=0.12 nm
Sn 2.0	Sb 2.1	Te 2.1

- **A highly mismatched alloy (HMA) is formed when anions are partially replaced with isovalent elements with distinctly different electronegativites and/or atomic radius**
  - $III\text{-}N_x\text{-}V_{1-x}$
  - $II\text{-}O_x\text{-}VI_{1-x}$
- Difficult to synthesize, large miscibility gaps

Energy gap vs. composition

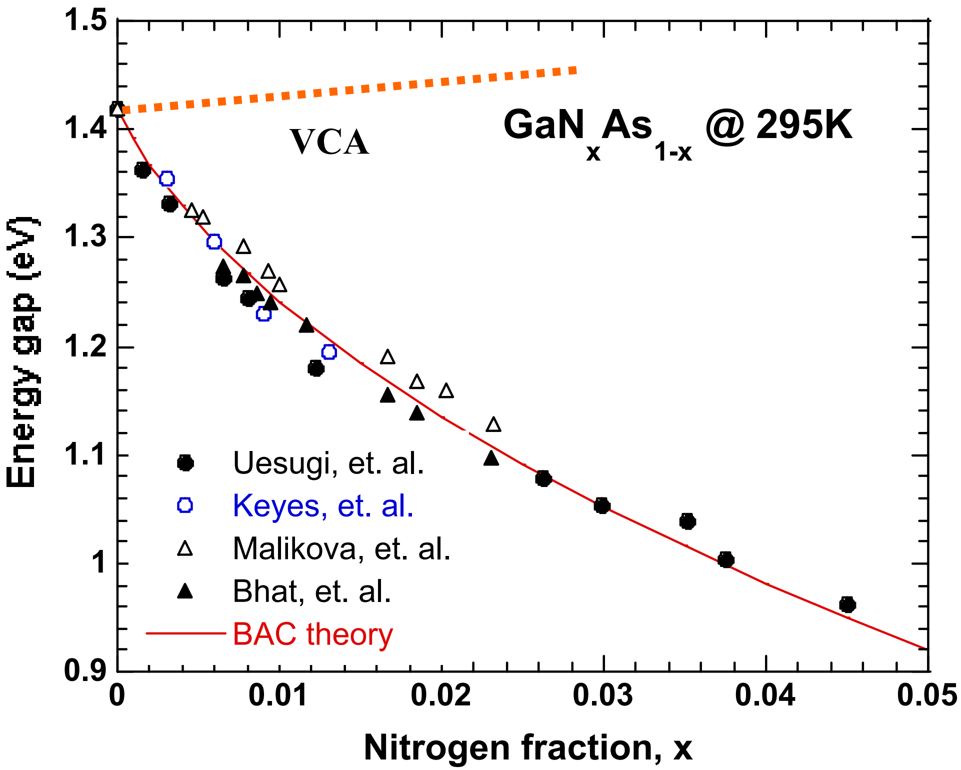

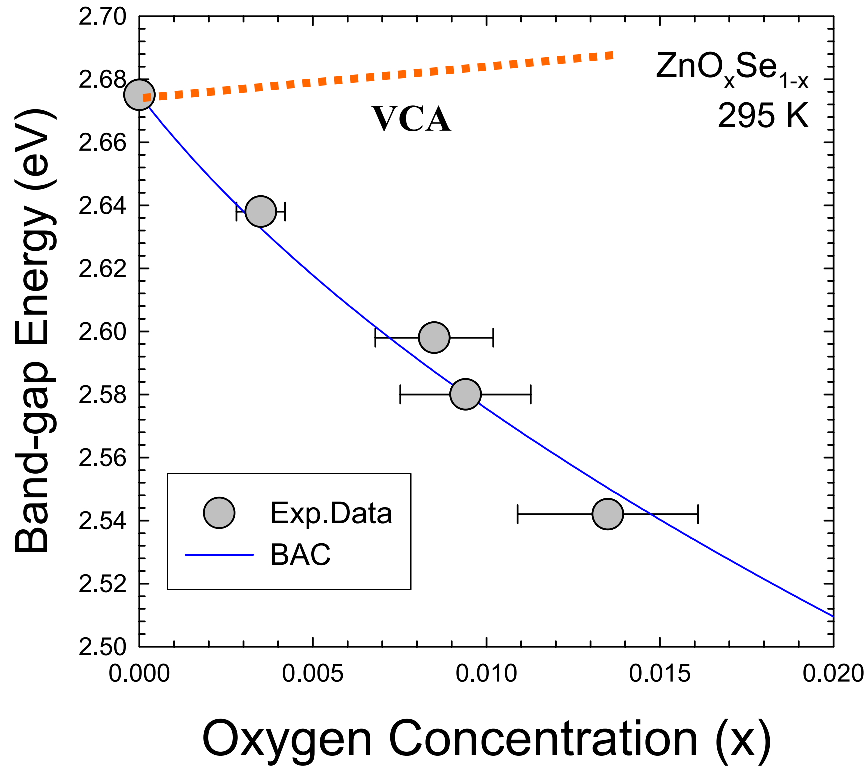

Huge deviation from VCA cannot be explained by constant bowing parameters

Dilute nitride alloys: $GaAs_{1-x}N_x$

- N level splits conduction band

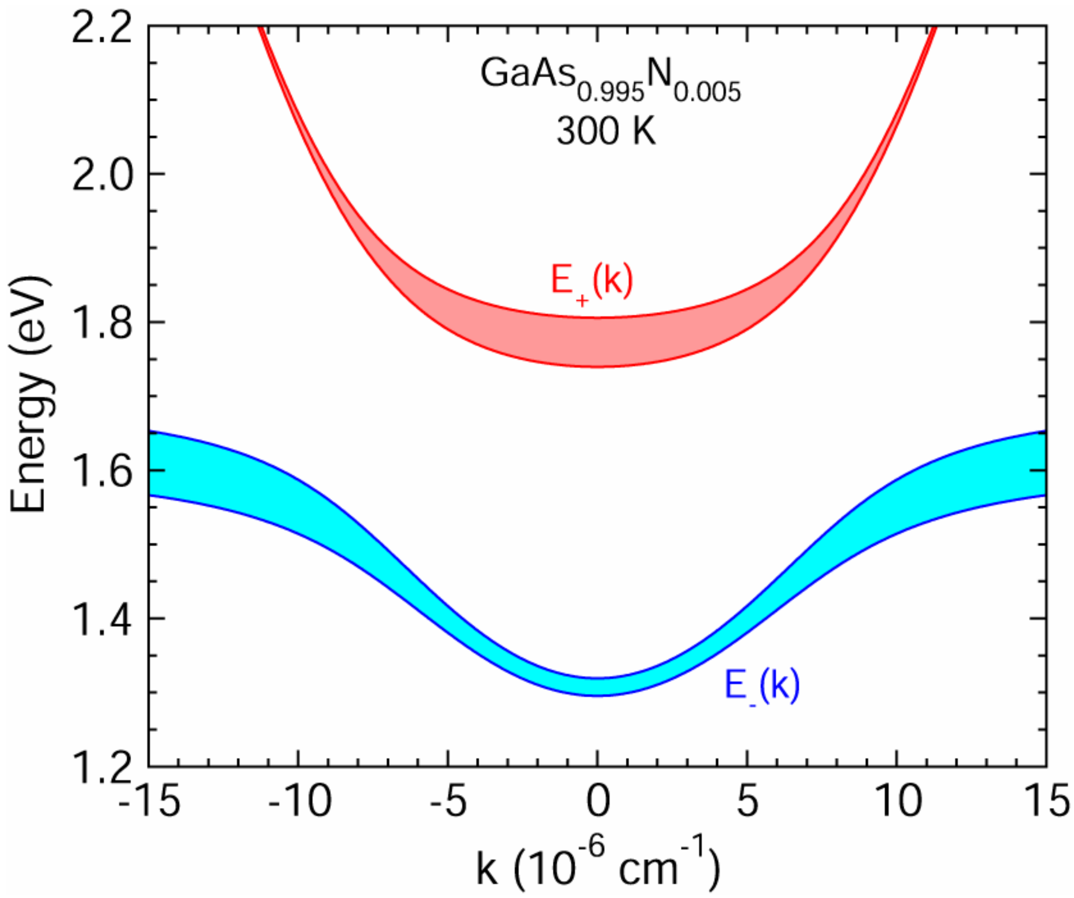

What happens if the local level is below the conduction band edge?

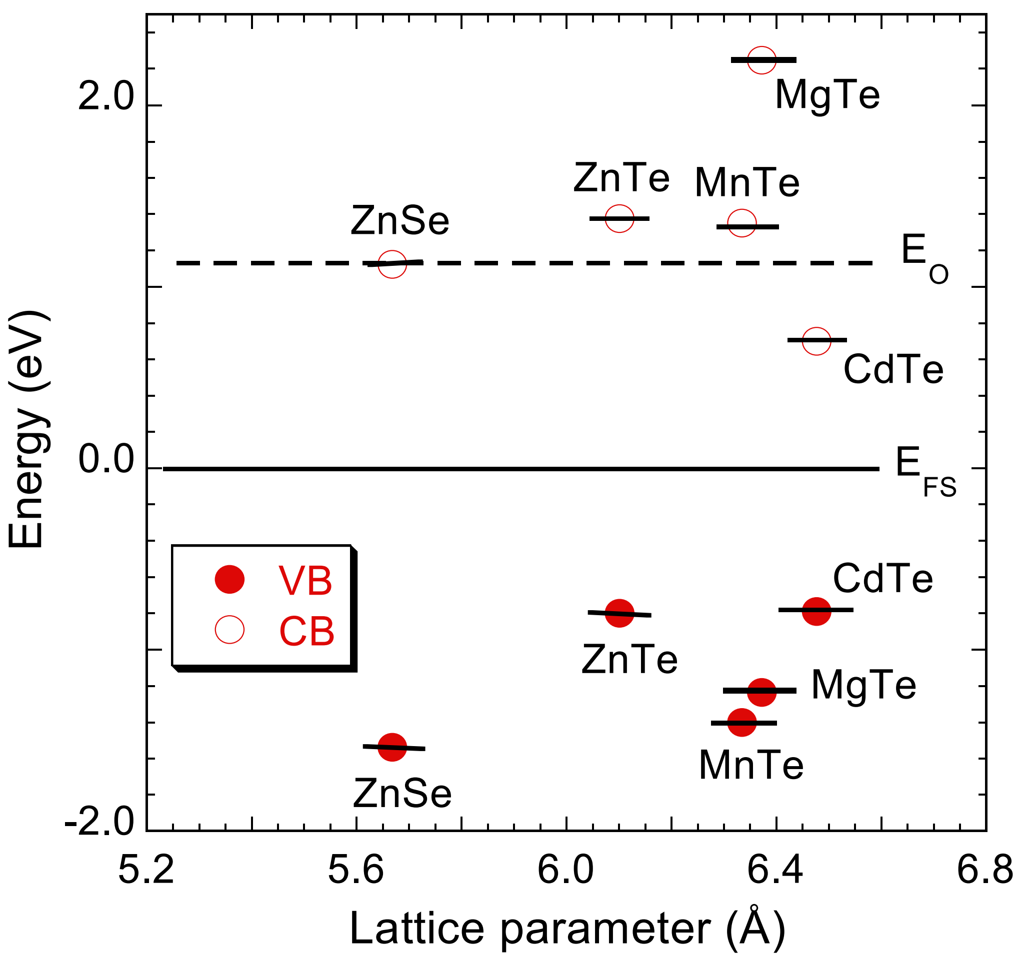

- Oxygen level in ZnTe is 0.24 eV <u>below</u> the conduction band (CB) edge
  - *Can be used to form an intermediate band*
- Synthesis challenges
  - Very low solid solubility limits of O in II-VI compounds
  - Nonequilibrium synthesis required
- *Very large mismatch!*

Synthesis of II-VI Oxide Alloys by Pulsed Laser Melting

Ion Implantation | **Pulsed Laser Melting** | **Thermal Annealing**

Pulsed excimer laser
KrF, 256 nm, 30 ns,
0.2-0.8 J/cm^2

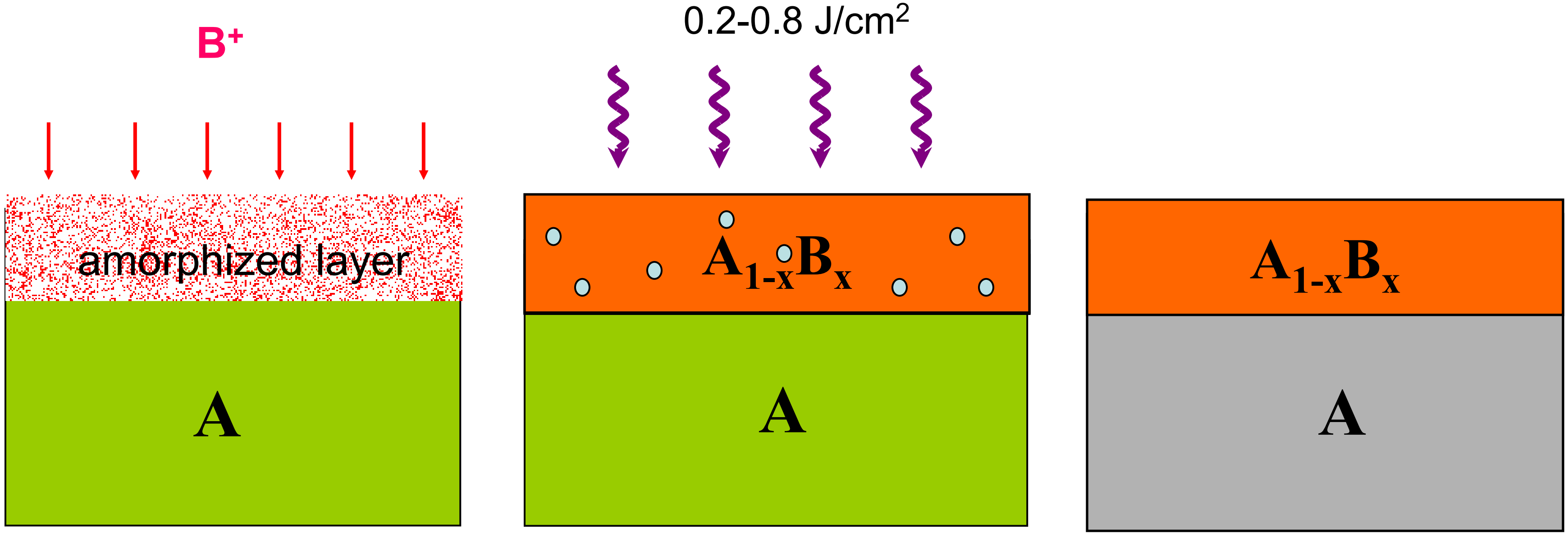

Ion Implantation

- multi-energy implantation results in uniform, amorphized thin layer

Pulsed Laser Melting

- epitaxial regrowth from undamaged substrate A
- melt duration & depth increase with laser fluence

Thermal Annealing

- Additional thermal annealing may be needed to remove point/line defects

Evidence of Subbands Formation in ZnMnOTe Alloys

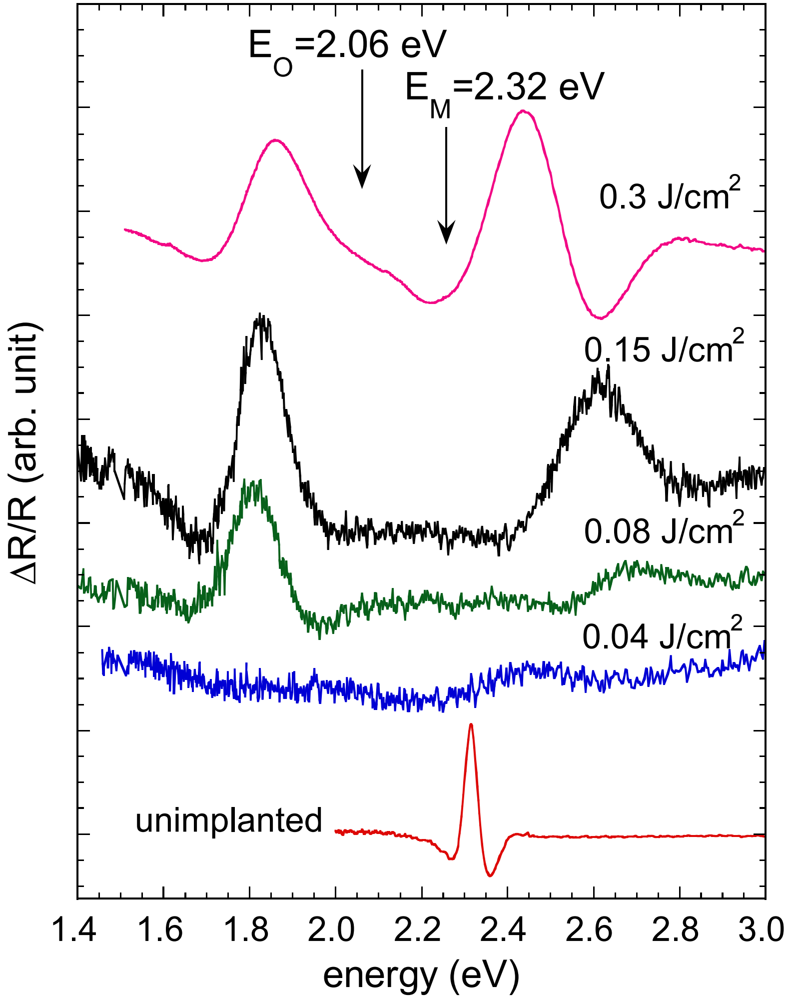

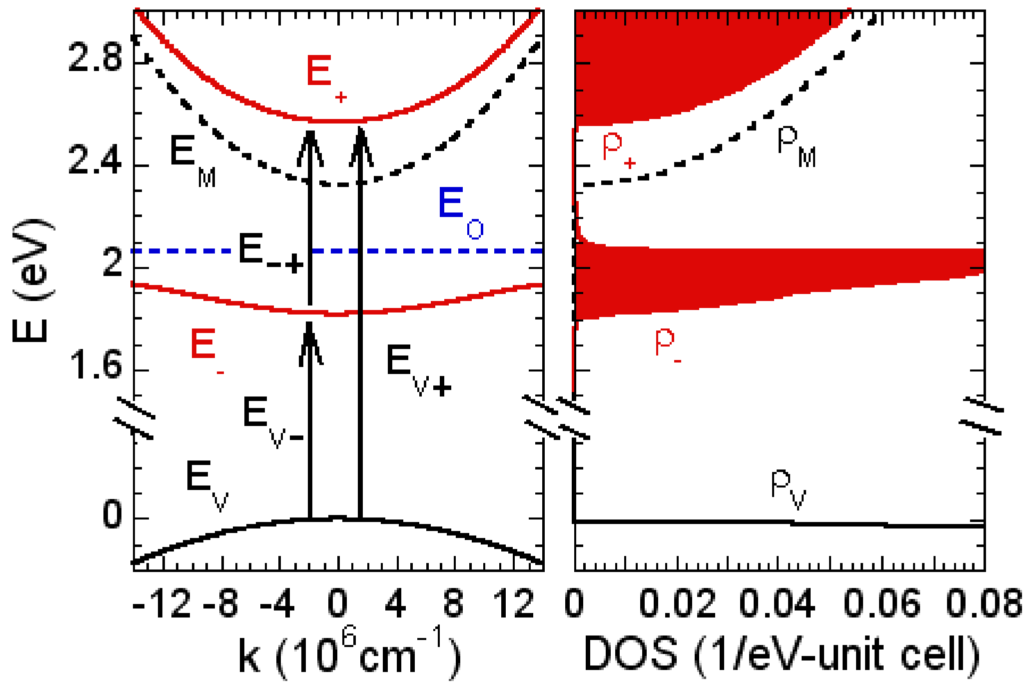

- Two sub conduction bands formed in ZnMnTe after oxygen implantation and PLM treatment.
- Extended nature and large density of states of both subbands as a result of BAC.

Photovoltaic Action

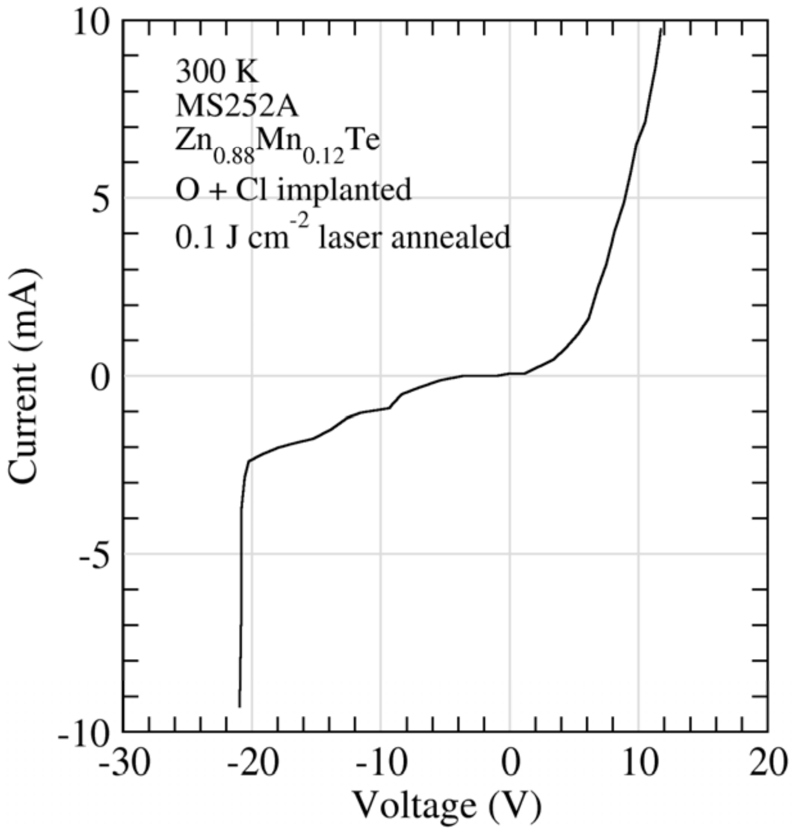

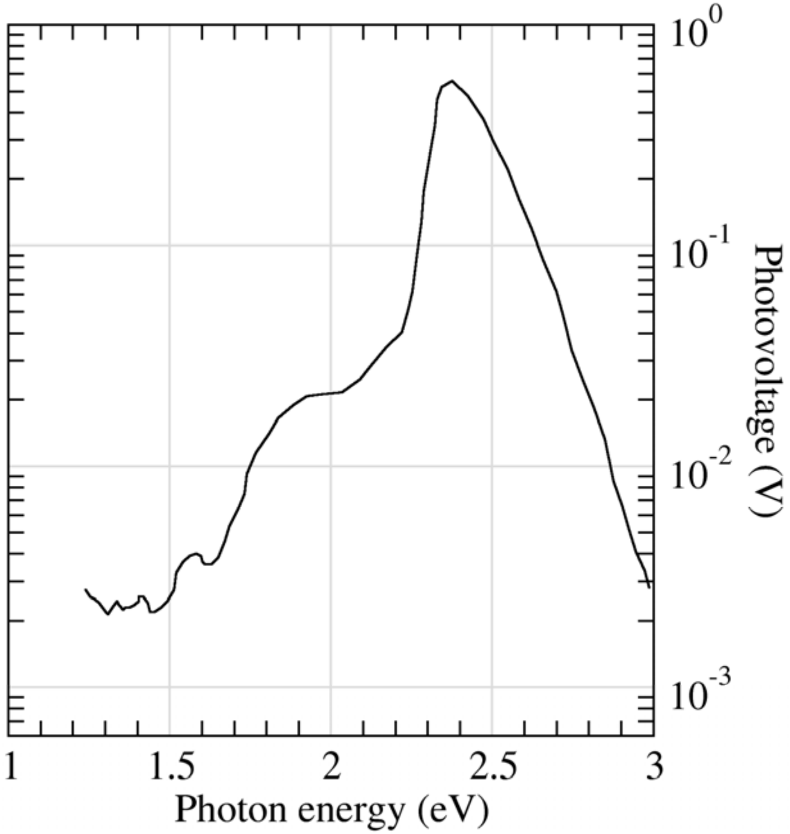

Solar to Hydrogen

ENERGY

VIEWPOINT

A Realizable Renewable Energy Future

John A. Turner

The ability of renewable resources to provide all of society's energy needs is shown by using the United States as an example. Various renewable systems are presented, and the issues of energy payback, carbon dioxide abatement, and energy storage are addressed. Pathways for renewable hydrogen generation are shown, and the implementation of hydrogen technologies into the energy infrastructure is presented. The question is asked, Should money and energy be spent on carbon dioxide sequestration, or should renewable resources be implemented instead.

Sustainable Paths to Hydrogen

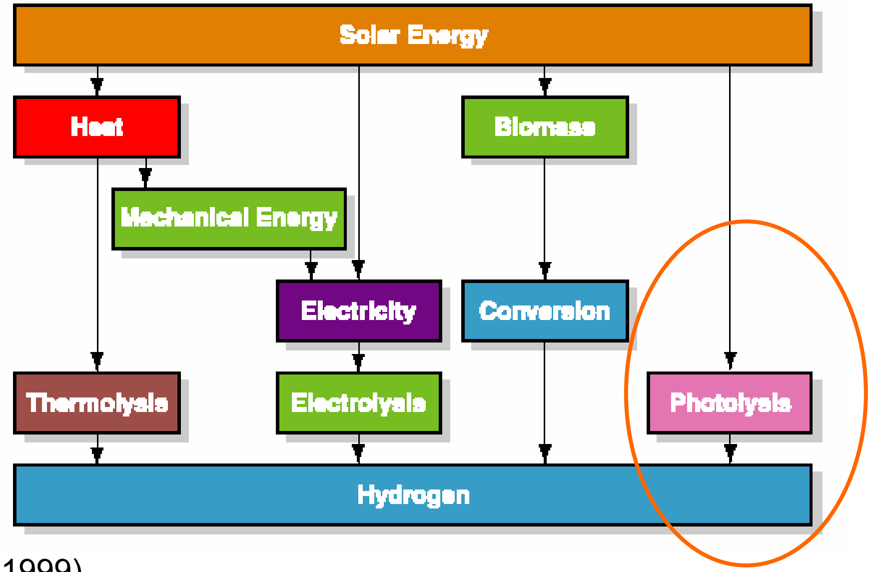

J. A. Turner, *Science* **285**, 687 (1999)

Photoelectrochemical H_2 generation

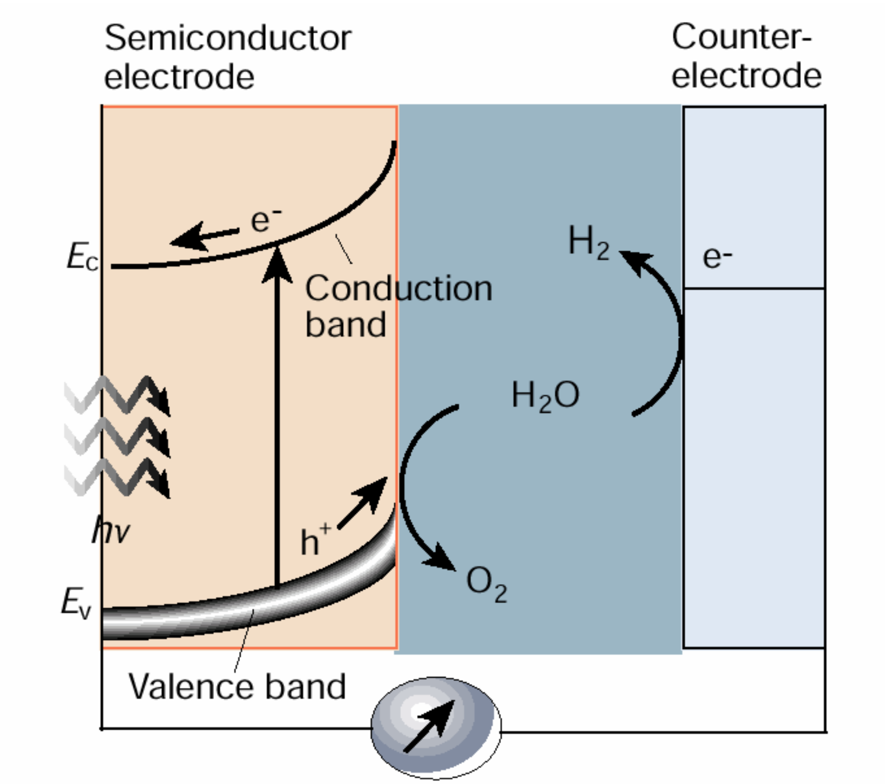

1. Absorption of light near the surface of the semiconductor creates electron-hole pairs.
2. Holes (minority carriers) drift to the surface of the semiconductor (the photo anode) where they react with water to produce oxygen:
   $2h^+ + H_2O \text{ -> } ½\ O_2\ (g) + 2H^+$
3. Electrons (majority carriers) are conducted to a metal electrode (typically Pt) where they combine with H^+ ions in the electrolyte solution to make H_2 :
   $2e^- + 2H^+ \text{ -> } H_2\ (g)$
4. Transport of H^+ from the anode to the cathode through the electrolyte completes the electrochemical circuit.

The overall reaction :

$2h\nu + H_2O \text{ -> } H_2(g) + ½\ O_2\ (g)$

Why is it hard to do?

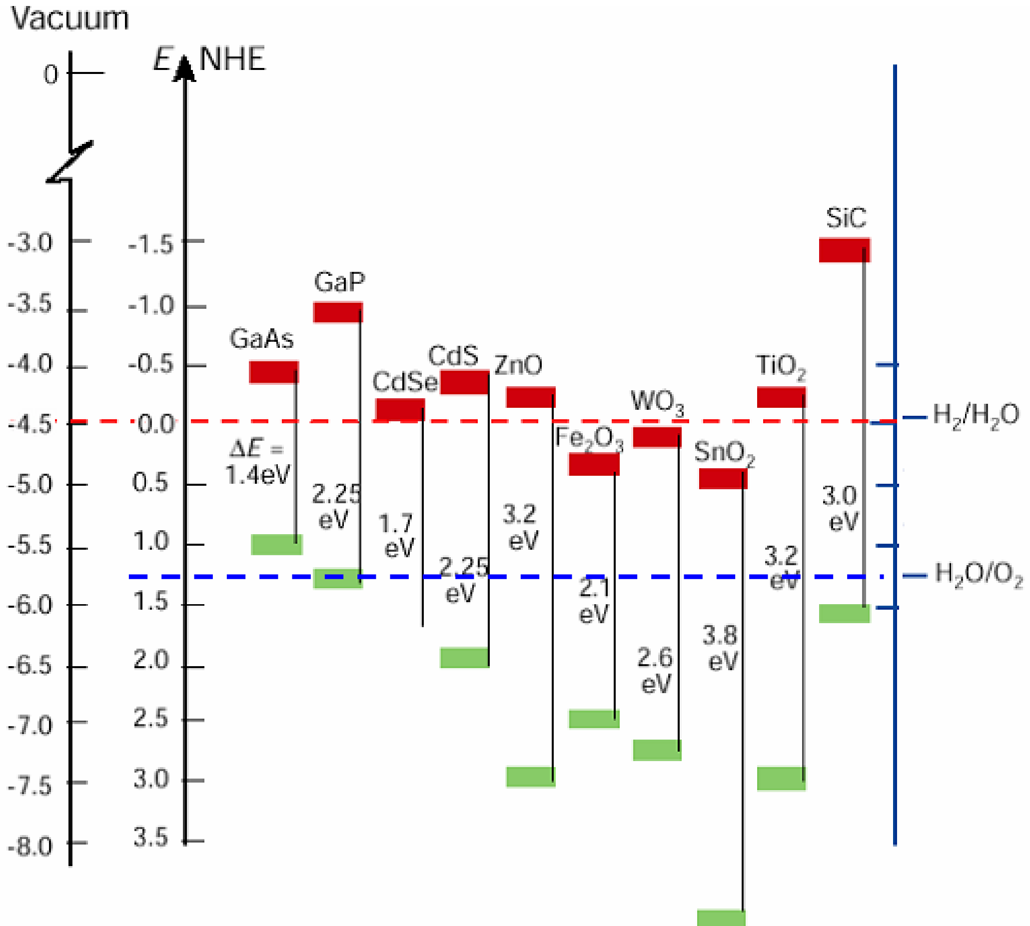

Adapted from M. Grätzel, *Nature* **414**, 388 (2001)

- Oxides
  - Stable but efficiency is low (large gap)
- III-Vs
  - Efficiency is good but surfaces corrode
- Approaches
  - Dye sensitization (lifetime issues)
  - Surface catalysis
- *No practical PEC H_2 production demonstrated*
  - *Efficiency <u>and</u> lifetime*

Engineering of the Band Offsets for Optimal PECs

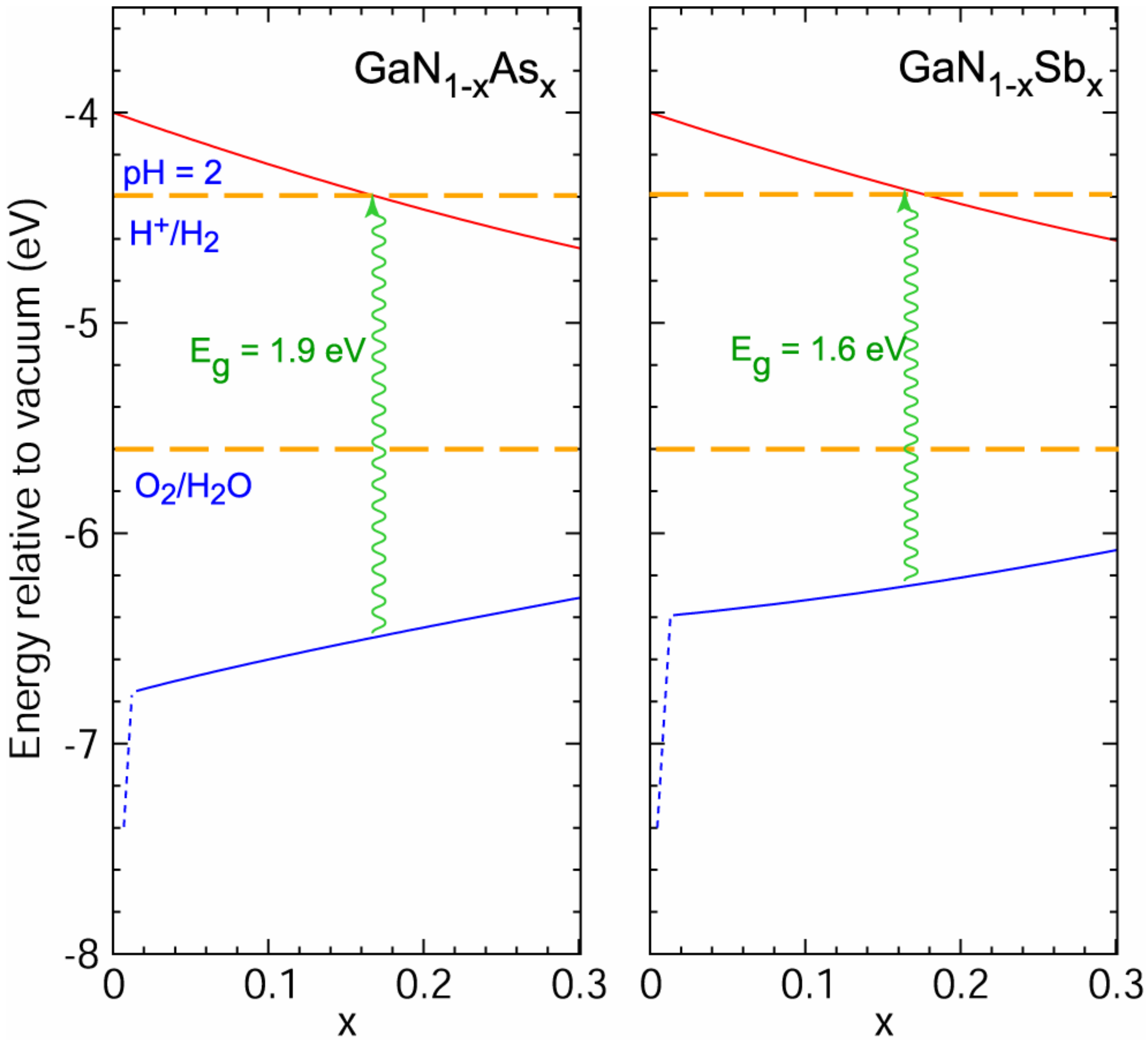

- In both $GaN_{1-x}As_x$ and $GaN_{1-x}Sb_x$ the valence band edge moves upward providing better match to O_2/H_2O potential
- CBM remains nearly unchanged as a function of *x*

Summary

- Electronic structure of InN and In-rich group III-nitride alloys is now well understood
- Significant progress in p-type doping of InN has been achieved
- $In_{1-x}Ga_xN$ and possibly also $In_{1-x}Al_xN$ alloys have potential for applications for high efficiency multijunction solar cells
- Large variety of highly mismatched alloys has been synthesized using ion implantation combined with pulsed laser melting.
- First intermediate band semiconductor has been demonstrated.
- ZnO_xTe_{1-x} alloys is a promising material for high efficiency intermediate band solar cells